Design and Analysis of a Liquid Nitrogen Delivery System for Cooling a High Temperature Superconducting Magnet for MAGLEV

by

Eric Fong

Submitted to the Department of Mechanical Engineering
in Partial Fulfillment of the Requirements for the
Degree of

Bachelor of Science

at the

Massachusetts Institute of Technology

June 1995

Signature of Author...
Department of Mechanical Engineering
May 12, 1995

Certified by...
Professor Richard D. Thornton
Thesis Supervisor

Accepted by...
Professor Peter Griffith
Chairman, Undergraduate Thesis Committee

Design and Analysis of a Liquid Nitrogen Delivery System for Cooling a High Temperature Superconducting Magnet for MAGLEV

by

Eric Fong

Submitted to the Department of Mechanical Engineering
on May 12, 1995, in partial fulfillment of the
requirements for the Degree of Bachelor of Science in
Mechanical Engineering

ABSTRACT

To maintain a cryogenic environment for an iron core high temperature superconducting magnet proposed for use in MAGLEV systems, a prototype liquid nitrogen (LN2) delivery system was designed, analyzed and constructed. A carbon based surface mount resistor with a negative thermal coefficient of resistivity of -269 ppm/K was used as a sensor to detect the level of LN2 inside a prototype cryostat and to maintain that level at a desired height of 2.4 cm above a prototype magnet. When the LN2 level fell below the desired height, the change in voltage of the sensor was detected by a Wheatstone bridge circuit. The LN2 delivery system would, in turn, be switched on by the circuit, filling the prototype cryostat until the desired height was attained.

Results from the initial theoretical analysis and computer simulations of the prototype LN2 delivery system did not accurately predict the operational dynamics of the prototype. Although the simulations proved that the delivery system would be able to reliably deliver LN2 and maintain the pace with the evaporation of LN2 from the cryostat, they also showed a considerable overshoot of LN2 into the cryostat, which was undesirable, and did not accurately predict the LN2 delivery and evaporation times. The prototype system, on the other hand, did not overshoot, and the desired LN2 level was maintained to within ± 1.5 mm.

Subsequent simulations using the actual LN2 volume flow rate into the cryostat and the actual LN2 evaporation rate from the cryostat produced more accurate results. This proved that the simulation model may be used to predict the operation of the prototype delivery system. Furthermore, the simulation model may be appropriately scaled up to predict the operation of a full scale LN2 delivery system, superconducting magnet and cryostat.

Thesis Supervisor: Professor Richard D. Thornton, Sc. D.

Title: Professor of Electrical Engineering

Acknowledgments

I would like to express my warmest thanks to the many people without whom I would not be able to complete this final undergraduate endeavor here in MIT.

First, I would like to thank Professor Richard Thornton for giving me the opportunity to pursue my interests and work on this project. I owe special thanks to Marc Thompson, who guided me in this study, taught me new skills, and just simply tolerated me for a whole term. To Ben Haid, I offer my appreciation for your answering the many questions I had concerning this project.

I am forever indebted to Stephen Lin and Esther Kim for allowing me to use their computers during the preparation of this thesis. They allowed me to take up their precious time even when they were busy with their own work.

All of my friends here in MIT, back home in New York and in Cornell University had to listen to me complain about writing this thesis. Some even helped me deal with my frustration. For all their help, I extend my deepest gratitude. I couldn't have done this without them.

Finally, I would like to thank my family for their support and encouragement all these years. They are the ones who made it possible for me to get to where I am today. No words can express how I feel about you all.

Contents

1. Introduction

1.1. Motivation for this Study

An iron core high temperature superconducting magnet has been proposed for use in MAGLEV systems [6]. A small-scale superconducting magnet, which will operate within a liquid nitrogen (LN2) bath at 77 K, is currently being designed. In support of such a system, several other components, or sub-systems, are essential. One of these components is a system to deliver the LN2 to the magnet containment vessel and to maintain the level of LN2 within the vessel at a required level.

The purpose of this current study is to design and test an LN2 delivery system for the small-scale superconducting magnet. The LN2 delivery system will be able to detect the height of the LN2 bath in the containment vessel, or cryostat. Should that LN2 height fall below a prescribed level, determined from other analyses, the delivery system will automatically feed LN2 into the cryostat until an ideal height has been reached. An analysis of this small-scale delivery system will determine how a larger version may be designed for the larger-scale superconducting magnet.

1.2. Goals of this Project

The objective of this project is to design and construct a reliable LN2 level detector and LN2 delivery pipe system for a prototype cryostat and prototype magnet. The level detector and delivery pipe system will be the main components of the prototype LN2 delivery system. Collectively, the prototype cryostat, magnet and LN2 delivery system is called the overall prototype system.

In support of such a design, a theoretical analysis of the dynamics of the overall prototype system will be done. The important considerations are the heat transfer involved in the cryostat, and the fluid dynamics of the LN2 delivery pipe system.

From the results of the theoretical analysis, simulations of the prototype system will be conducted to determine its performance. The theoretical

analysis and simulation results will be used in the actual design of the LN2 delivery system.

Finally, a full scale version of the LN2 delivery system will be proposed for use with a full scale cryostat and superconducting magnet.

1.3. Format of this Thesis

The following report begins with an explanation of the theoretical analysis of the overall prototype system. The results from the theoretical analysis are presented afterwards. This is followed by the design of the components of the prototype system and description of the experimental procedure involved in testing the LN2 delivery system. A discussion of the theoretical and experimental results and recommendations for further work concludes the main body of this report. The appendices at the end contain further technical information and mathematical analyses involved in this study.

2. Theoretical Analysis

To determine the dynamics of the liquid nitrogen delivery system, small scale magnet and prototype cryostat without the use of a full physical setup, a mathematical model of the system is derived based upon the principles of physics, heat and mass transfer, and fluid dynamics. Computer simulation of this mathematical model will produce theoretical results that may be compared with results obtained from actual experiments with the physical setup. The accuracy of the theoretical results compared to the experimental results will determine if the mathematical and simulation models are reliable in describing the overall prototype system. If the mathematical and simulation models are accurate to within an acceptable percentage, then the models may be used as the basis of a theoretical representation of a larger cryostat and magnet system.

2.1. Relationship Between Electrical Resistance and Temperature

Several ideas for detecting and/or measuring the level of liquid nitrogen inside the cryostat had been considered. Indeed, liquid level detectors are commercially available. However, these are usually expensive devices. The ideal level detector for this sort of project must satisfy several requirements. One requirement is cost: the device need not be an expensive one. A second requirement is sensitivity: the device should be able to detect the level of liquid nitrogen to within the desired tolerance. Reliability is another factor because the device must be able to perform its function properly at 77 K, the boiling temperature of liquid nitrogen.

Because of the cost factor, commercially available liquid level detectors for cryogenic applications were not considered for this project. Having investigated several kinds of detecting or sensing devices, it was decided that the electrical resistor satisfied the design requirements better than the other devices.

Resistors are relatively inexpensive devices and are readily available. Ordinary resistors can function in 77 K as well as 300 K (room temperature). The small size of a resistor makes them well suited to applications in which size is a factor. Resistors are also easy to calibrate and to use [3, pp. 159].

Common carbon resistors are sensitive to temperature variations. Their electrical resistance increases as the temperature decreases. Thus, they have a negative thermal coefficient of resistivity. In comparison, most metals have a positive thermal coefficient of resistivity: their resistance decreases as the temperature decreases.

If the change in resistance of a resistor is large as the temperature is varied between 77 K and 300 K, the change may be easily detected either by directly measuring the resistance with an ohm-meter type device, or by passing a current through the resistor and measuring the voltage change. However, if the change in resistance is relatively small, perhaps only a few ohms, then it would be easier to measure a voltage change rather than a resistance change. By applying a large enough current through the resistor, the voltage change may be large enough to comfortably detect.

In this project, the main concern is to maintain the level of liquid nitrogen inside a cryostat at a predetermined height. By fixing a physically small resistor inside the cryostat at the desired height, it will be easy to detect

whether the liquid nitrogen is above or below that height. If the liquid nitrogen is above the desired level, the resistor will be within the liquid nitrogen bath and have the resistance value corresponding to 77 K. Once the liquid nitrogen drops below the desired height and the resistor is outside of the bath, the resistance value will decrease until it reaches a value corresponding to a higher temperature. This is the simplest method by which to detect the level of the liquid nitrogen.

However, if the time it takes the resistor to change its resistance in either direction is too long, the detection of the liquid nitrogen level becomes less accurate. When a resistor, initially at 300 K, is immersed in liquid nitrogen, the heat in the resistor is quickly carried away by the LN2, which has a high thermal capacity. Thus, the time it takes for the resistor to transition from 300 K to 77 K will be negligibly short. However, when the resistor is taken out of the LN2 bath, the time it takes to transition from 77 K to 300 K will be much longer than the transition time in immersing the resistor into LN2. This is because air has a low thermal capacity, and thus it takes longer for the resistor to warm. However, by running a current though the resistor, the joule heating can overcome any time delays in the temperature variation. The faster the resistor warms from 77 K to 300 K, the faster the resistance transitions. This leads to a more accurate detection of the level of LN2, as less LN2 evaporates before the resistor detects that the LN2 has fallen below the desired height.

2.2. Heat Transfer of the Prototype Cryostat

Before a system can be designed to maintain the level of LN2 inside the prototype cryostat at a predetermined height, the heat transfer that is associated with the cryostat must first be understood. From this understanding, the rate at which LN2 evaporates may be calculated, and the appropriate LN2 delivery system may be then be designed.

2.2.1. Joule Heating from the Magnetic Coils

The small-scale, prototype magnetic coils for the overall MAGLEV project had already been designed and constructed prior to the research and design of

the LN2 delivery system. Figure 1 shows a dimensioned diagram of the magnet. It is made from copper wire coiled around an iron laminated core.

Copper Coil Magnet for the Prototypte Cryostat

(Top View)

7.40 cm

3.80 cm

Copper Magnet Coil

11.00 cm

1/8" thick G-10 Fiberglass Panel

25.00 cm

7.80 cm

8.60 cm

24.20 cm

(Front View)

Iron Laminate Core

(Side View)
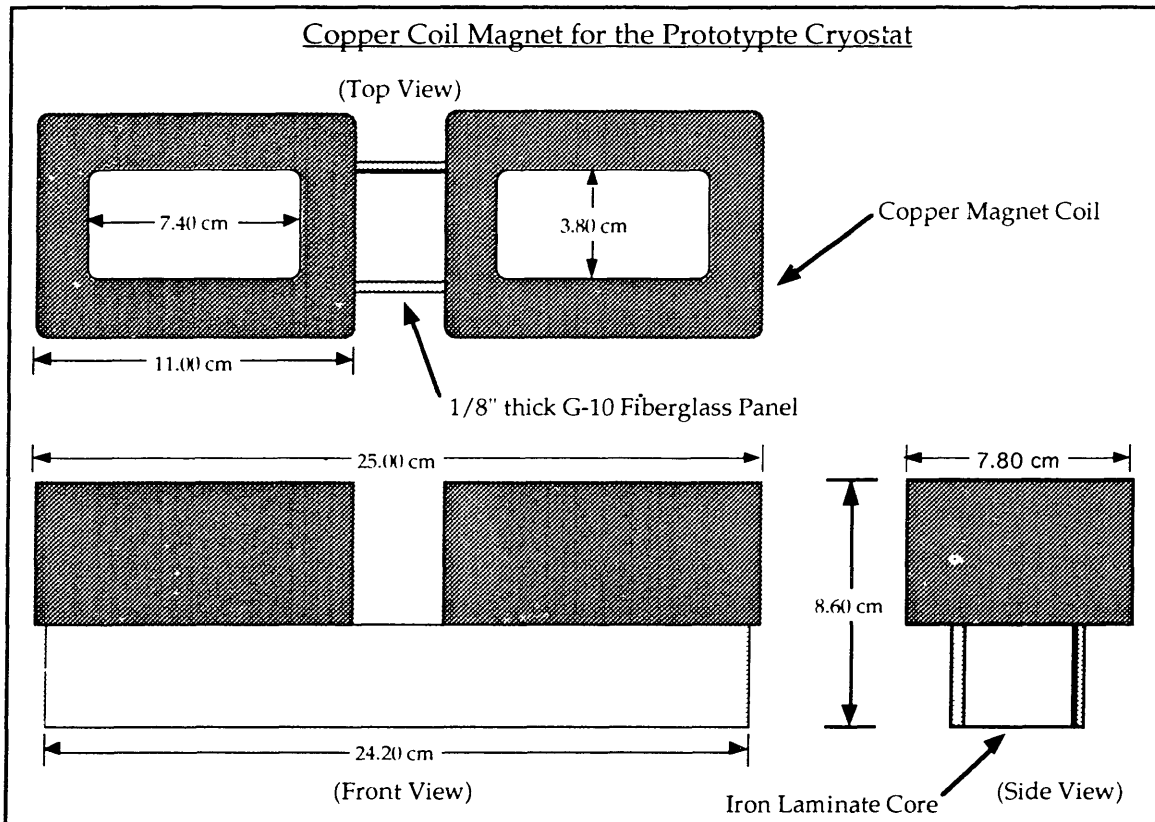
Figure 1: Small scale magnet tested in the prototype liquid nitrogen (LN2) cryostat.

During operation, a DC current is applied to the two copper coils, which are in series. From Joule's law, the power dissipation, P, from a resistor of resistance R with a current I is:

$$P = I^2R \qquad (1)$$

Because copper has a positive thermal coefficient of resistivity, the resistance of the copper coils will decrease as the temperature of the coils decreases from 300 K to 77 K in the LN2 bath. It is the resistance at 77 K that should be used in Equation 1. The power, P, is the rate at which energy, in the form of heat, is dissipated to the LN2 bath.

2.2.2. Conduction Heat Transfer through the Prototype Cryostat

The prototype cryostat and copper magnet system that is used in the lab to simulate the larger cryostat and full scale superconducting magnet must maintain a cryogenic environment. However, the liquid nitrogen bath is subjected to considerable heat transfer from its external environment, which includes the cryostat and the ambient 300 K air surrounding the cryostat. The amount of heat transferred to the internal liquid nitrogen bath through the cryostat, plus the power dissipation from the copper magnet, determines the LN2 evaporation rate. By knowing the evaporation rate, an appropriate LN2 delivery system may be designed and constructed to maintain a stable cryogenic environment for the magnet.

The specific heat transfer processes that must be analyzed are radiation, convection, and conduction. However, a complete understanding of the heat transfer processes involved in this system is beyond the scope of this study. Rather, the goal of this study is to arrive at an approximate answer to the heat transfer analysis. Therefore, a simplified model of the dynamic heat transfer processes that occur is studied instead. From a preliminary analysis, there is enough information to conclude that the single most significant heat dissipation process involves heat conduction. Thus, it is assumed that heat transfer through thermal radiation and thermal convection is negligible.

Thermal radiation is the process by which a solid surface at a finite temperature higher than its surroundings emits energy to lower its temperature and achieve thermal equilibrium with its surroundings.[1] Within the cryostat, the entire magnet and the portion of every surface of the cryostat in contact with LN2 is at 77 K when in equilibrium.[2] Because these surfaces are not at a higher temperature than their LN2 surroundings, there should not be any radiation from these surfaces. However, there is a gap, between the LN2 surface and the top face of the cryostat, that is occupied by nitrogen vapor. Thus, through the process of heat convection, which is discussed below, there exists a temperature gradient in the vapor. The vapor

---

[1]In this analysis, only thermal radiation from a solid surface will be considered. However, energy emission may also occur from liquids and gases [2, pp. 9].

[2]By equilibrium, it is meant that after the magnet and the surfaces in contact with LN2 have cooled down to 77 K. This happens after the magnet and the surfaces have been bathed in LN2 long enough for their internal energy to decrease through heat transfer to the LN2.

10

closest to the LN2 surface is at a temperature very close to 77 K, and the vapor near the cryostat surfaces is at a temperature higher than 77 K. For simplicity, it is assumed that the cryostat is a completely sealed and that the temperature gradient in the vapor is negligible. With this assumption, the cryostat surfaces that are not directly in contact with LN2 will still be considered to be at 77 K. Thus, there will be no thermal radiation from the internal cryostat surfaces or the magnet to the LN2.

Thermal convection refers to the mode of heat transfer in which energy is exchanged between a surface and a moving fluid when they are at different temperatures. A temperature gradient exists in the region of fluid at the surface, as the temperature varies from the surface temperature T_S at the surface to the prevailing temperature T_F in the outer flow. This region is called the thermal boundary layer. If $T_F > T_S$, the heat transfer is to the surface. If $T_F < T_S$, the heat transfer is to the fluid. The convective heat flux q'' (W/m^2) is proportional to the difference between the fluid temperature and the surface temperature, and is expressed by Newton's law of cooling:

$$q'' = h(T_S - T_F) \qquad (2)$$

The constant of proportionality h ($W/m^2 K$) is called the convection heat transfer coefficient, and it encompasses all the parameters that affects convection heat transfer. Some of the more important parameters include the conditions in the boundary layer, surface geometry, the nature of the fluid flow, and various fluid thermodynamic and transport properties. Any study of convection ultimately focuses on a means to determine h.

For the prototype cryostat system, convection heat transfer occurs on the outside surfaces of the cryostat, with the surrounding air at 300 K as the fluid in question, and also on the inside surfaces of the cryostat, with a thin layer of nitrogen vapor separating the inside surfaces and the LN2 as the corresponding fluid in motion. However, because the convection heat transfer coefficients for the outside and the inside convection processes are not known, and their investigation is beyond the scope of this research, convection is assumed to be negligible. Studying the convection process will only aid in determining the inside and the outside surface temperatures. Thus, in neglecting thermal convection, the inside surface temperature is assumed to be 77 K, and the outside surface temperature is assumed to be 300 K. These are reasonable assumptions because thermal convection acts as a

11

thermal resistance, lowering the overall heat transfer through the cryostat walls. In fact, a complete convection analysis would reveal that the outside surface temperature is lower than the surrounding air temperature of 300 K, and that the inside surface temperature is higher than the LN2 temperature of 77 K. This reduces the temperature differential through the cryostat walls, decreasing the overall heat transfer. Thus, the upper limit for the heat flux q" through the cryostat is defined by assuming 300 K and 77 K for the surface temperatures on the outside and on the inside, respectively.

This leaves thermal conduction through the cryostat walls as the only heat transfer process affecting the prototype cryostat system. Conduction is the transfer of energy through a medium due to a temperature gradient in the substance. The energy flows from the higher temperature (thus, higher energy) particles of the substance to the lower temperature particles. The conductive heat flux q" (W/m^2) through a one-dimensional plane wall is given by Fourier's law:

$$q" = k\frac{T_1 - T_2}{L} \tag{3}$$

where T_1 and T_2 are the surface temperatures ($T_1 > T_2$), L is the wall thickness, and k (W/mK) is the thermal conductivity of the wall substance. Since heat flux is the heat transfer rate q (W) per unit area A perpendicular to the direction of transfer, the heat rate q may be expressed as:

$$q = q"xA \tag{4}$$

Figure 2 shows a cross-sectional view of the prototype cryostat wall. All six walls of the cryostat are constructed of a G10 fiberglass panel on the inside, and a Styrofoam (polystyrene) panel on the outside.[3] For overall structure, the cryostat is surrounded by a box made from thin, clear plastic.[4] However, for simplicity, it is assumed that the plastic structure does not affect the conduction heat transfer, and is thus neglected in the analysis.

It is necessary to determine the temperature of the interface, T_i, between the G10 and the polystyrene in order to calculate the conductive heat rate q_c. Since the heat flux through the polystyrene, $q"_P$, is equal to the heat flux through the G10, $q"_G$, Equation 3 may be applied accordingly to determine T_i:

---

[3]For the remainder of this report, styrofoam will be referred to by its scientific name, polystyrene.
[4]Please see the Section 4.2 for a more detailed description of the small cryostat.

$$k_P \frac{T_a - T_i}{L_P} = k_G \frac{T_i - T_n}{L_G} \qquad (5)$$

where k_P and k_G are the thermal conductivities of polystyrene and G10, respectively, $T_a = 300$ K is the assumed outside surface temperature of the polystyrene, $T_n = 77$ K is the assumed inside surface temperature of the G10, and L_P and L_G are the thicknesses of the polystyrene and the G10, respectively. Upon rearranging Equation 5, T_i is determined by:

$$T_i = \frac{\dfrac{k_P T_a}{L_P} + \dfrac{k_G T_n}{L_G}}{\dfrac{k_P}{L_P} + \dfrac{k_G}{L_G}} \qquad (6)$$

The intermediate temperature T_i is the same for each face of the prototype cryostat because every wall is identical.
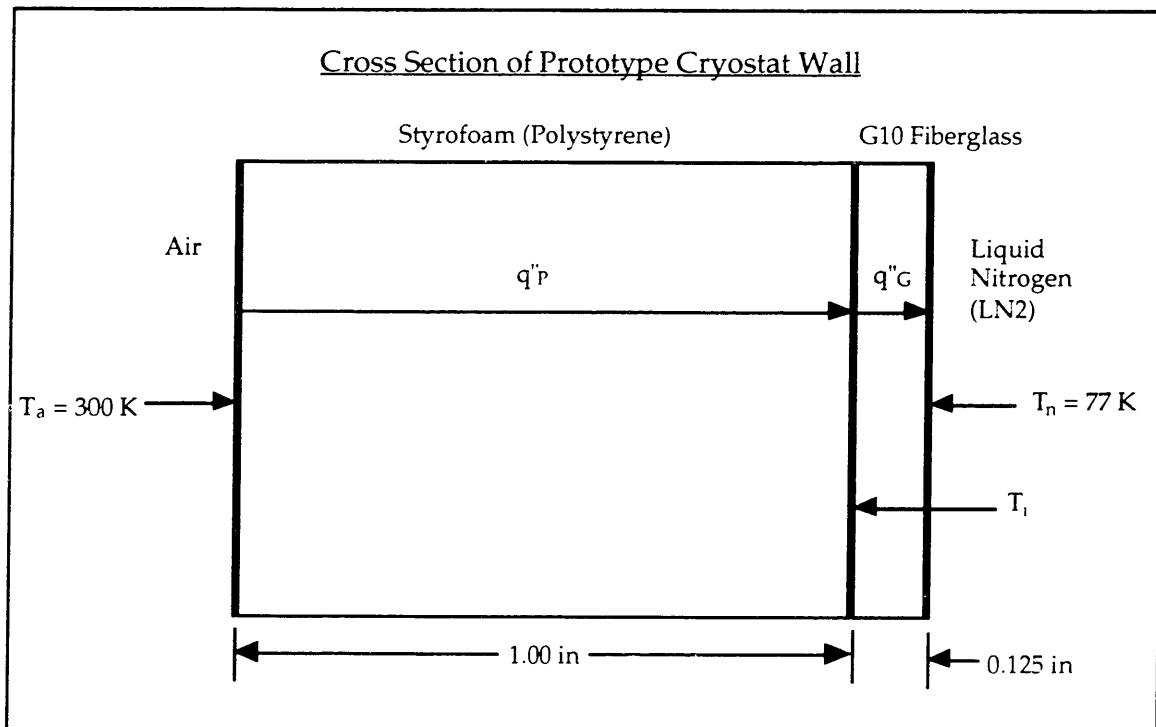

Figure 2: Model of the prototype cryostat wall used in the conduction heat transfer analysis.

The conductive heat rate, q, through each wall, according to Equation 4, is equal to the heat flux, q", times the area, A, perpendicular to the direction of heat flow. The overall conductive heat rate, q_C, through the entire cryostat is equal to the sum of the heat rates through each wall. Since by Equation 3 the heat flux, q", through each wall is the same, then q_C and the power dissipation by conduction, P_C , is determined by combining Equation 3 and Equation 4:

$$P_C = q_C = \frac{k_G A_\Gamma (T_i - T_n)}{L_G} = \frac{k_P A_T (T_a - T_i)}{L_P} \tag{7}$$

where A_T is the sum of the surface areas of each face of the cryostat.

2.2.3.   Evaporation Rate of Liquid Nitrogen

The total power dissipation, P_T, to the LN2 bath determines the evaporation rate of LN2. The sum of the power dissipation from the copper magnets, P_M, given by Equation 1, and the power dissipation from thermal conduction, P_C, is equal to P_T:

$$P_T = P_M + P_C \tag{8}$$

The rate of LN2 evaporation, m'_e, in volume per second, is given by the following equation:

$$m'_e = \frac{P_T}{h_L} \tag{9}$$

where h_L (J/cm^3) is the latent heat of vaporization of liquid nitrogen. The latent heat of vaporization is the energy required for a phase change at the surface of a liquid.

2.3.   Liquid Nitrogen Flow Rate and Pipe Time Delay

The rate at which liquid nitrogen flows into the prototype cryostat is determined by the various components in the LN2 delivery system. Figure 3 shows how the system was modeled for the flow analysis.[5] Beginning with the fundamentals of fluid dynamics, an equation that describes the LN2 flow

---

[5]For a more detailed description of the LN2 delivery system, see the Section 4.3.

14

may be derived. By knowing the flow rate and the dimensions of the pipes used in the delivery system, the time delay associated with the delivery system may be determined.
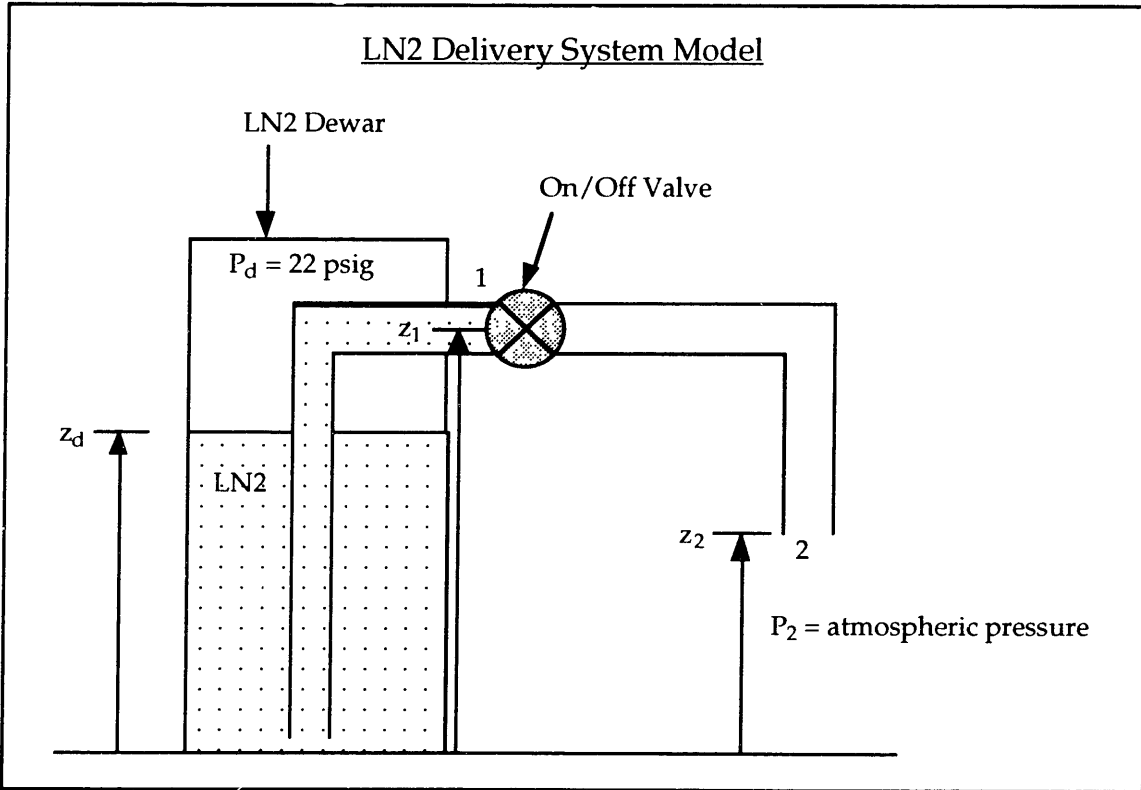

Figure 3: Model of the LN2 delivery system used in the flow rate analysis.

To theoretically arrive at an equation for the flow rate, the LN2 and the physical setup of the delivery system must be idealized. The LN2 is modeled as an incompressible and inviscid fluid. The flow is assumed to be steady flow. From the idealized model of the delivery system, two sources of head loss are identified. They are the pressure loss across the on/off valve and the pressure loss around the 90° bend in the pipe. The pressure loss, ΔP_v, across the on/off valve is given by:

$$\Delta P_v = \frac{Q}{K_v} = \frac{AV}{K_v} \tag{10}$$

where K_v (m^3/sPa) is the valve loss coefficient, Q is the volume flow rate, A is the cross-sectional area of the pipe, and V is the fluid velocity entering the valve. The pressure loss, ΔP_b, corresponding to the 90° bend is given by:

$$\Delta P_b = \rho C \frac{V^2}{2} \qquad \qquad (\;.)$$

where C is the loss coefficient for a bend, V is the fluid velocity leaving the bend, and ρ is the density of the fluid.

Having idealized the fluid flow and identified the sources of head loss, the delivery system may now be mathematically modeled by combining Equation 10 and Equation 11 with Bernoulli's equation for inviscid, incompressible, steady flow:

$$\frac{P_1}{\rho} + \frac{V_1^2}{2} + g z_1 = \frac{P_2}{\rho} + \frac{V_2^2}{2} + g z_2 + \frac{AV_1}{K_v \rho} + C\frac{V_2^2}{2\rho} \qquad (12)$$

This equation is applied to a fluid streamline from point 1 to point 2. The gravitational constant is g, and z_1 and z_2 are the height of points 1 and 2.

The velocity of the fluid entering point 1 is determined by applying Bernoulli's equation to a streamline within the dewar and assuming the downward velocity of the fluid level inside the dewar is negligible ($V \approx 0$ m/s) compared to the fluid velocity leaving the dewar at point 1. Thus, the equation for V_1 is:

$$V_1 = \sqrt{2\left[\left(\frac{P_d - P_1}{\rho}\right) + g\left(z_d - z_1\right)\right]} \qquad (13)$$

where P_d is the internal absolute pressure of the dewar, and z_d is the height of the LN2 level inside the dewar.

Upon rearranging Equation 12, the velocity of the fluid leaving point 2 is thus:

$$V_2 = \sqrt{\frac{2}{C+1}\left[\frac{P_1 - P_2}{\rho} + \frac{V_1^2}{2} - \frac{AV_1}{K_v \rho} + g\left(z_1 - z_2\right)\right]} \qquad (14)$$

By knowing the velocity of the fluid, V_2, leaving the delivery system and the area of the delivery pipe, the volume flow rate, m'_f, of the fluid may be determined. Furthermore, knowing V_2 and the length, l, of the delivery pipe determines the time delay for the overall delivery system.[6]

---

[6]It is assumed that the time it takes the LN2 to leave the dewar is negligible compared to the time it takes the LN2 to travel through the valve and delivery pipe.

3. Theoretical Results

From the various equations derived in the theoretical analysis of the prototype system, numerical parameters that describe the system were calculated. Using the Matlab and Simulink numerical computation and visualization software available on the MIT Athena computing environment, a block diagram model that would simulate the prototype system was constructed. The parameters were entered into the block diagram model, and the simulation produced LN2 height-versus-time and LN2 flow rate-versus-time profiles. These profiles described how the prototype system functioned over time.

3.1. Evaporation Rate, LN2 Flow Rate and Pipe Time Delay

Aside from the physical dimensions of the prototype system, the essential parameters required for the Matlab simulation are the evaporation rate of LN2 from the prototype cryostat, the rate at which LN2 flows into the cryostat everytime the delivery system automatically switches on, and the time delay between the delivery system turning on and when the LN2 reaches the cryostat.

Equation 8 and Equation 9 determines the LN2 evaporation rate, m'_e. The parameters used in the calculation of the total power dissipation, P_T, are given in Table 1, for use in calculating the copper magnet power dissipation from Equation 1, and in Table 2, for use in calculating the heat transfer power dissipation from Equation 7. As shown in Table 1, the maximum current that will run through the prototype magnets is 10 amps. From previous experiments, each copper magnet coil exhibited a resistance of 0.445 ohms at 77 K. Although Table 2 lists the relevant parameters for both the G10 fiberglass panel and the polystyrene panel, either set of parameters may be used in calculating the heat transfer power dissipation.

Table 1: Parameters for calculating the magnet power dissipation.

Parameter	Value
Number of Magnet Coils	2
Current, I	10 amps

Coil Resistance, R	0.445 ohms

Table 2: Parameters for calculating the heat transfer power dissipation.

Parameter	G10 Fiberglass	Polystyrene
Thermal Conductivity[7], k	k_G = 0.56 W/mK	k_P = 0.022 W/mK
Total Area $\perp$ to Heat Flow, A_T	0.17 m^2	0.17 m^2
Temp. of Initial Surface[8], T_1	T_i = 78.09 K	T_a = 300 K
Temp. of Terminal Surface, T_2	T_n = 77 K	T_i = 78.09 K
Thickness, L	3.175x10^{-3} m (1/8 inch)	0.0254 m (1 inch)

Table 3 lists the results of the LN2 evaporation rate calculations. The total power dissipation from the magnets and from the heat transfer through the walls of the prototype cryostat is P_T = 121.67 watts. This results in an LN2 evaporation rate of m'_e = 0.76 cm^3/s.

Table 3: Power dissipation and LN2 evaporation rate for the prototype system.

Power Dissipation from Magnets, P_M	89 W
Power Dissipation from Heat Transfer, P_C	32.67 W
Total Power Dissipation, P_T	121.67 W
LN2 Latent Heat of Vaporization[9], h_L	161 J/cm^3

---

[7]For the thermal conductivity of G10 fiberglass between 80 and 300 Kelvin, see [3, pp. 140]. For that of polystyrene, see [7, pp. I-96 to I-97].

[8]The temperature of the interface, T_i, between the G10 fiberglass and the polystyrene is calculated from Equation 6.

[9]See [3, pp. 112].

LN2 Evaporation Rate, m'_e	0.76 cm^3/s

In determining the volume flow rate of LN2 from the prototype delivery system, the LN2 velocity, V_1, leaving the dewar and the LN2 velocity, V_2, leaving the end of the delivery pipe must be known. Table 4 shows the relevant parameters for solving for V_1 from Equation 13. Because the velocity of LN2 leaving the dewar when the dewar is full ($z_d = z_1$) and the velocity when the dewar is almost empty ($z_d \approx 0$) differs by only 0.8 m/s, the average of the two velocities is taken to be the V_1 used in solving for V_2. Table 5 shows the parameters used in solving for V_2 from Equation 14.

Table 4: Parameters for solving V_1, the LN2 velocity exiting the dewar.

Parameter	Value
Dewar Pressure, P_d	253 KPa absolute (22 psig)
Exit Pressure, P_1	101.3 KPa (atm. pressure)
LN2 Density[10] (@ 77K), ρ	807 kg/m^3
Height of Exit Nozzle, z_1	1.524 m (5 feet)
Height of LN2 in Dewar, z_d	1.524 m (dewar full) 0 m (dewar empty)

Table 5: Parameters for solving V_2, the LN2 velocity exiting the delivery system.

Parameter	Value
Pressure at Valve Entrance, P_1	253 KPa absolute (22 psig)
Pressure at Pipe Exit, P_2	101.3 KPa (atm. pressure)
Loss Coefficient of Valve[11], K_v	9.06x10^{-9} m^3/sPa (0.99 GPM/psi)

---

[10]See [3, pp. 383]
[11]Taken from manufacturer's specifications in Grainger Catalogue.

Loss Coefficient of 90° Bend[12], C	2
Pipe Area, A	7.13×10^{-5} m^2 (3/8 inch inner diameter)
LN2 Density (@ 77 K), ρ	807 kg/m^3
Height of Valve Entrance, z_1	1.524 m (5 feet)
Height of Pipe Exit, z_2	1.224 m (4 feet)

The total pipe length in the prototype delivery system was 0.6 m (2 feet). Thus, from knowing V_1 and V_2, the LN2 volume flow rate, m'_f, and the delivery system's time delay, T_D, may be determined. The results are summarized in Table 6. The prototype LN2 delivery system theoretically has a volume flow rate of $m'_f = 794.28$ cm^3/s, and a time delay of $T_D = 0.054$ s.

Table 6: LN2 volume flow rate and time delay for the prototype LN2 delivery system.

Dewar Exit Velocity, V_1	19 m/s
Delivery System Exit Velocity, V_2	11.14 m/s
Pipe Area, A	7.13×10^{-5} m^2 (3/8 inch inner diameter)
Total Pipe Length, l	0.6 m (2 feet)
LN2 Volume Flow Rate, m'_f	794.28 cm^3/s
Delivery System Time Delay, T_D	0.054 s

3.2. Prototype System Simulation

Using the Matlab and Simulink numerical computation and visualization software on the MIT Athena computing environment, a block system representation of the entire prototype system, which includes the LN2

---

[12]See [1, pp. 520]

delivery system, the cryostat, and the magnets, was designed for the simulation. From the simulations, information concerning the height of the LN2 level inside the cryostat and the LN2 evaporation and flow rates during operation of the prototype was obtained. The simulation results were used to predict the operation of the prototype. Comparisons with the results from a real test of the prototype system would determine if the block representation on Simulink is reliable in modeling the prototype system and, subsequently, a full scale version of the prototype.

Figure 4 shows the Simulink block representation of the prototype system.[13] The parameters essential to the simulations were the dimensions of the cryostat, the desired LN2 height, the LN2 detector and the on/off valve time constants, the delivery system time delay, and the rates of LN2 flow and evaporation. The objective of the simulation was to maintain the LN2 level to within ± 1 mm. Table 7 lists the theoretical parameters entered into the simulation. The on/off valve and the LN2 sensor time constants, τ, were obtained from observations and tests of the valve and sensor.

Table 7: Parameters for the initial simulation of the prototype system based on theoretical values.

Parameter	Value
LN2 Volume Flow Rate, m'_f	794.28 cm^3/s
LN2 Volume Evaporation Rate, m'_e	0.76 cm^3/s
LN2 Height, h	11 cm
Pipe Delay, T_D	0.054 s
On/Off Valve Time Constant, τ_v	0.1 s
LN2 Level Detector Time Constant, τ_s	0.31 s
Ideal LN2 Bath Volume, V_b	3378.76 cm^3

---

[13]See Appendix 8.1 for an explanation of the Simulink simulations.

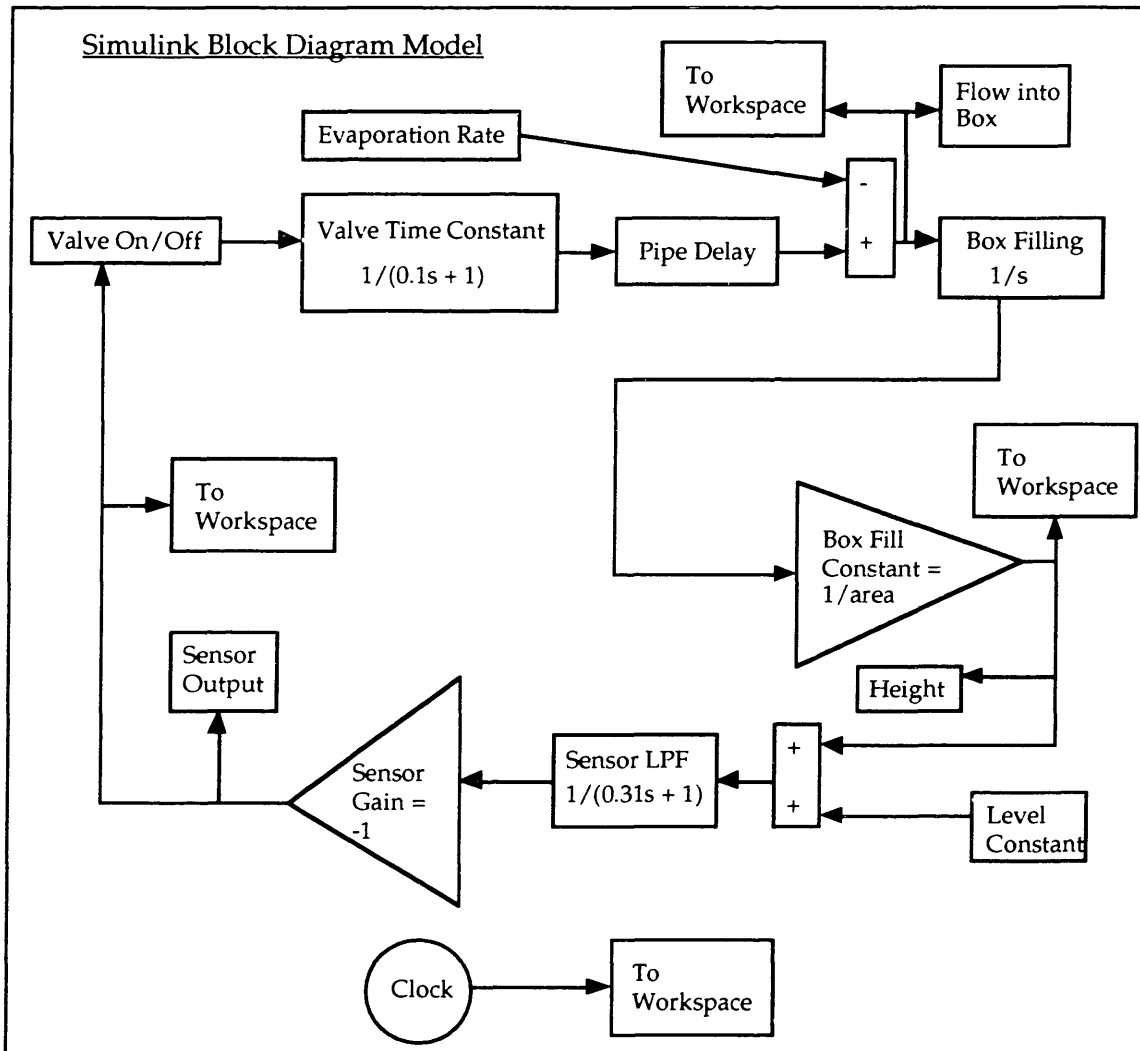| Box Fill Constant (1/Area)	3.26x10^{-3} m^{-2}

Figure 4: Simulink block diagram model used to simulate the overall prototype system.

The simulation time was 250 seconds. Profiles of the LN2 height and the LN2 flow rate into (from the delivery system) and out of (due to evaporation) of the prototype cryostat are shown in Figure 5.

The initial simulation results showed that the LN2 level sensor detected that the LN2 level fell 1-2 mm below the ideal height of 11 cm. The delivery system switched on for less than one second, allowing the LN2 height to reach 12 cm before stopping the flow. The subsequent LN2 evaporation from

the cryostat lasted longer than 200 seconds before the level reached 11 cm again. These results were later compared with the results from a test of the prototype system. Section 6 discusses the simulation and the test results in more detail.

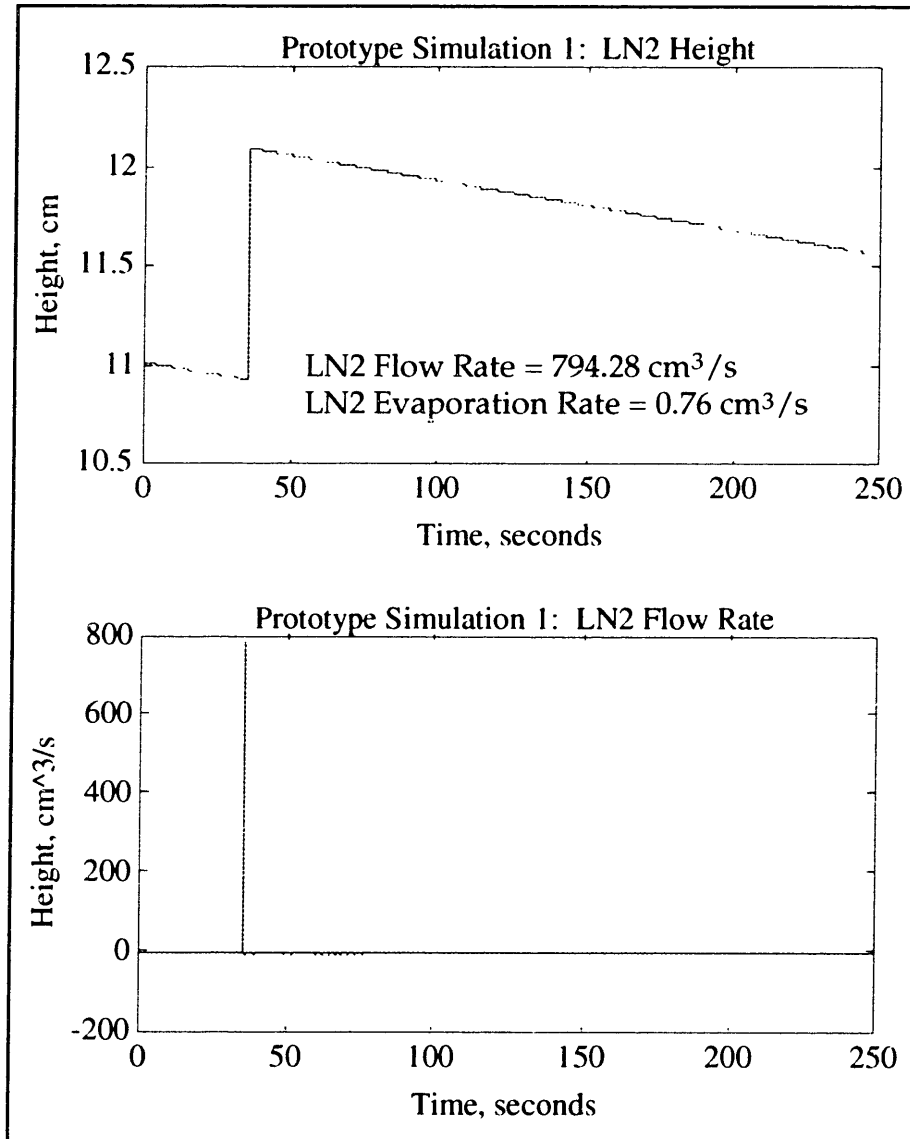Figure 5: Initial simulation results using theoretically calculated parameters.

4. Design and Apparatus

The cryostat and magnet for the prototype system had already been constructed prior to this current study. Thus, the remaining component of

the prototype system that was designed in this project is the LN2 delivery system. The LN2 delivery system may be separated into the LN2 level detector electronics and the LN2 delivery pipe system.

4.1. Overall system diagram

Figure 6 shows a diagram of the overall prototype system. It consists of the cryostat, the copper coil magnet, the LN2 level detector, and the LN2 delivery system. During operation, the magnet sits within an LN2 bath inside the cryostat, and is connected to an adjustable DC current source. The LN2 level detector circuitry is located outside the cryostat, but the actual sensor is inside. The detector is connected to the LN2 delivery system via a solenoid valve. The end of the delivery pipe feeds into the cryostat through a small entrance in the cryostat top.
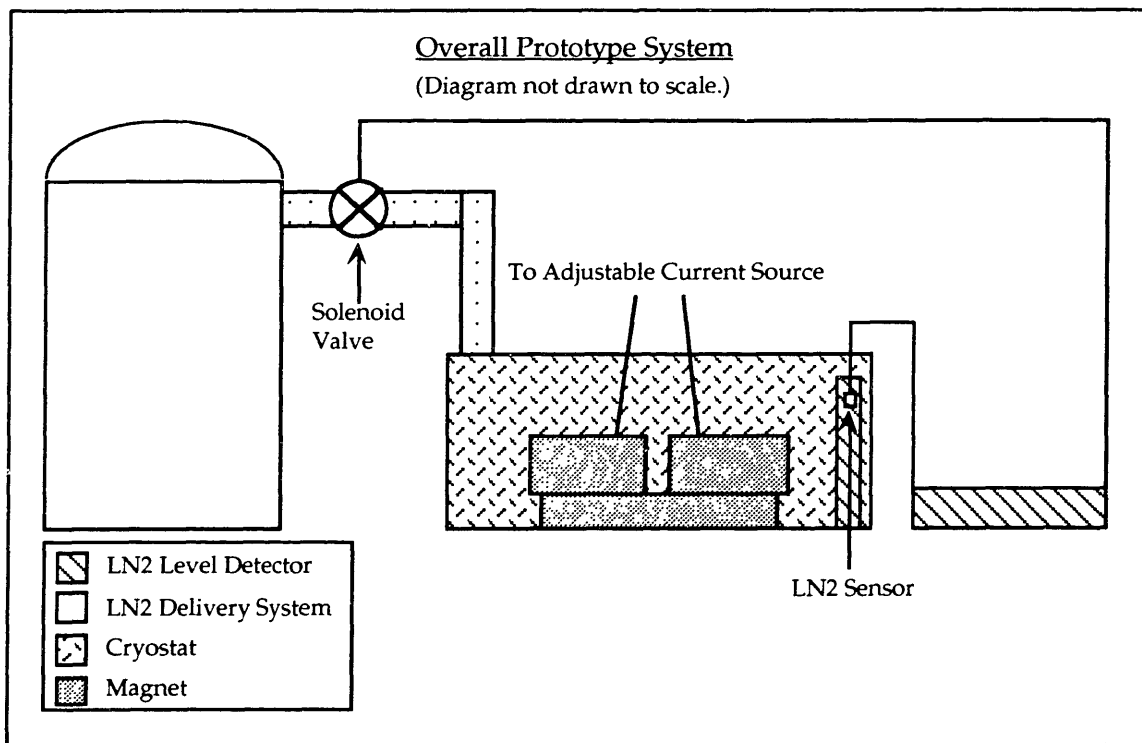
Figure 6: Diagram of the overall prototype system setup.

4.2. Prototype Cryostat and Magnet

F shows a diagram of the prototype LN2 cryostat. It is constructed with 1/8" thick G10 fiberglass panels on the inside, and 1" thick polystyrene panels

24

on the outside. Refer to Figure 2 for the cross section of the cryostat wall. The top is removable to allow the magnet and LN2 sensor to be taken out of the cryostat.
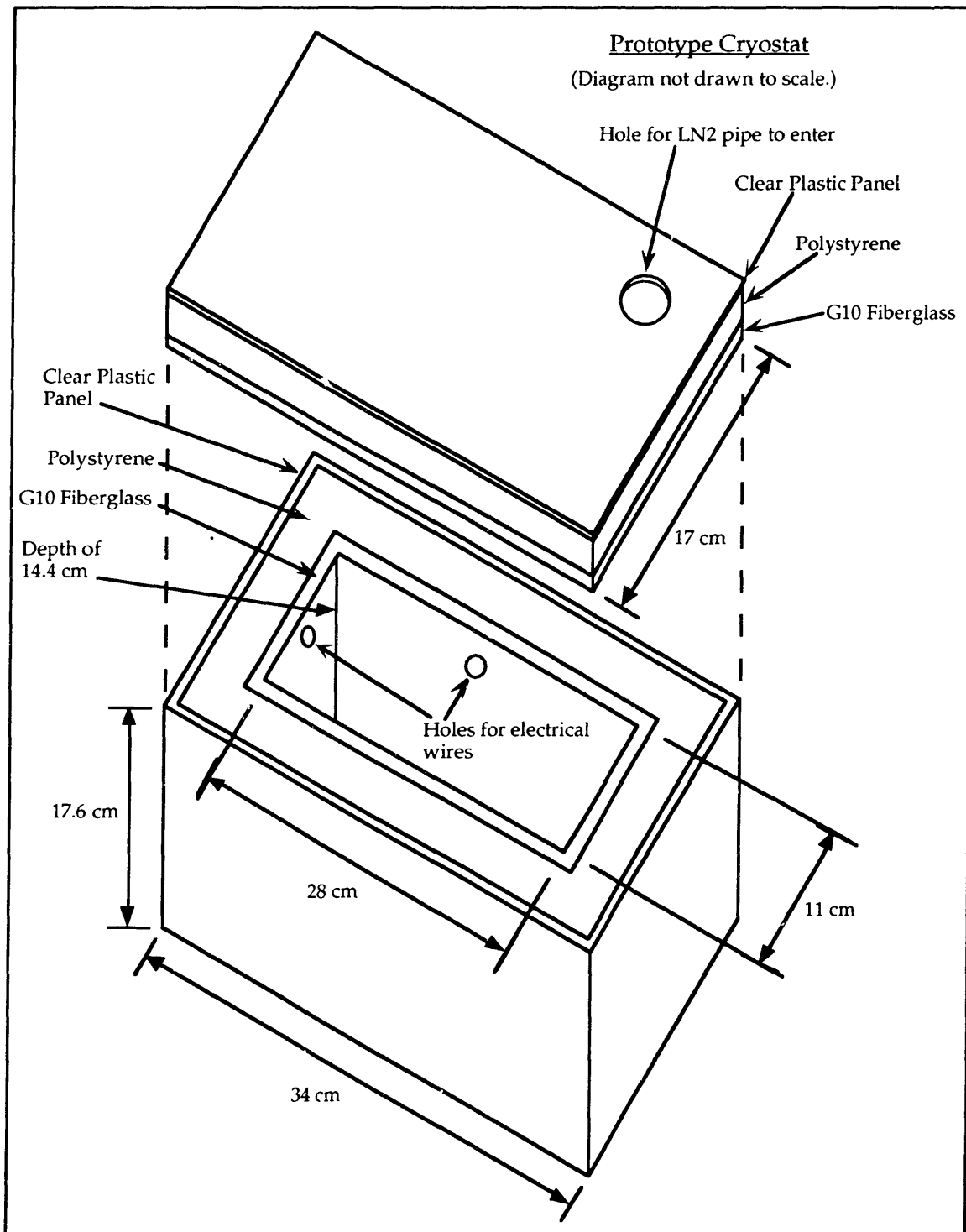

Figure 7: The prototype LN2 cryostat.

G10 fiberglass is a common structural material for cryogenic applications. It has high tensile and compressive strength, and low thermal conductivity over a temperature range [3, pp. 140]. It is also a lightweight material. In comparison, although steel has much higher strength, it also has a high thermal conductivity.

The G10 fiberglass box on the inside of the cryostat is made from five panels held together and sealed using fiberglass cloth and Stycast 2850 epoxy adhesive. The sixth panel is used for the removable top. To insulate the cryostat, polystyrene is epoxied to the G10. For overall structure, the cryostat is further held together by a box constructed from clear plastic panels.

There is a 1.25 inch diameter hole at one corner of the cryostat top for the LN2 delivery system's feed pipe to enter. Near the top of two adjacent sides of the cryostat is a 0.5 inch diameter hole for electrical wires and other leads to enter. The leads are for powering the magnet and for taking measurements.

Due to cost, the copper coil magnet is used in this prototype to simulate a superconducting magnet [6, pp. 15]. Refer to Figure 1 for a diagram of the copper magnet. The magnet core is made from iron laminations. There are two coils in this prototype magnet.

4.3. LN2 Delivery System

4.3.1. Designing the LN2 Level Detector

Based on the fact that carbon resistors change resistance due to a change in temperature, the method chosen to detect the LN2 level is to measure the voltage of a carbon resistor sensor and compare that against a known fixed voltage. The set point of the fixed voltage is within the voltage variation range of the carbon resistor. Since carbon resistors have a negative thermal coefficient of resistivity, the voltage of the sensor outside of LN2 is higher than the voltage of the sensor within LN2. When the sensor voltage decreases to below the set point voltage, the LN2 level is below the sensor and the level detector switches the LN2 delivery system on. If the sensor voltage increases to above the set point voltage, the LN2 level has filled to above the sensor and the level detector switches the delivery system off.

4.3.1.1.   Selecting the Resistor for the Sensor

In selecting the appropriate resistor for the sensor, the main considerations are the range of resistance variation between 77 K and 300 K, power dissipation, resistor size and resistor time constant.   A large resistance variation range is necessary to ensure that, given a low input current, the associated voltage range is large enough to detect. Using a low input current to the resistor limits the amount of power dissipation from the resistor. This is important because high power dissipation may change the performance of the resistor (i.e., decrease the resistance variation range or increase the resistor's time constant).   The physical size of the resistor must be small so that the height of the LN2 level may be detected to within a tighter tolerance. The time constant of the resistor must also be small so that changes in the LN2 level may be detected quicker, leading to tighter tolerance in the level.

Carbon surface mount resistors and carbon composition resistors were tested for their resistance variation range and for their time constant.   Each resistor has a 1/4 watt power dissipation capacity.   A diagram of a surface mount resistor is shown in Figure 8.   The carbon composition resistors are the common resistors found in laboratories.   The surface mount resistor values (at 300 K) tested were 100 Ω, 300 Ω, and 820 Ω, and the carbon composition resistor values tested were 100 Ω and 1.8 kΩ.[14]

The 300 Ω surface mount resistor is chosen for the LN2 sensor because, although its resistance variation range is not as large as the other resistors, it has the fastest time constant and the smallest physical size. The time it takes the other types of resistors to switch from their low resistance value at 300 K to their high resistance value at 77 K is on the order of three seconds. The 300 Ω resistor takes less than one second to switch from its room temperature value to 318 Ω at 77 K. The 18 Ω range, or more accurately the associated voltage range, for this resistor is large enough to detect, even with low input currents.   Furthermore, the surface mount resistors are smaller than the carbon composition resistors. This will help in maintaining a small tolerance in the LN2 height.

---

[14]See Appendix 8.2 for an explanation of the tests and the test data.

Surface Mount Resistor
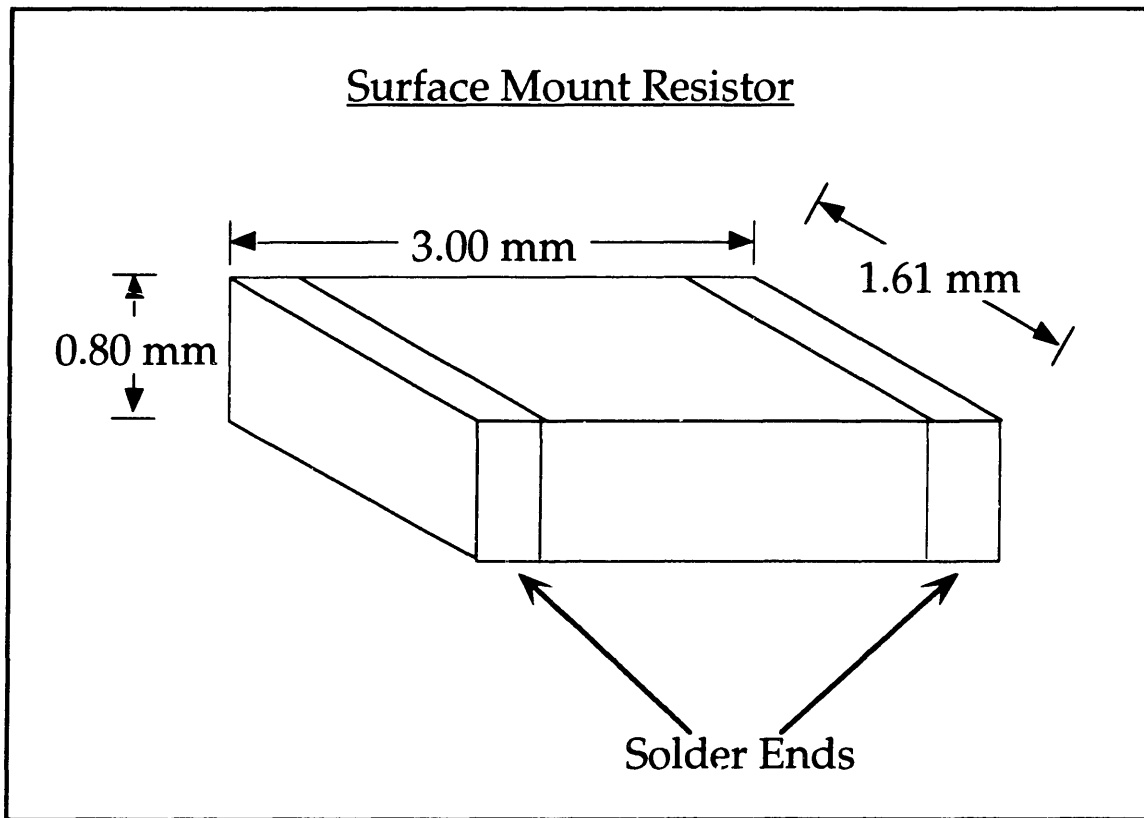
3.00 mm

1.61 mm

0.80 mm

Solder Ends

Figure 8: Surface mount resistor.

4.3.1.2. Designing the Circuitry

Figure 9 shows a circuit diagram of the LN2 level detector. The circuit is powered by a +15 volt source. A +5 volt source is also established by an LM78L05 voltage regulator from the +15 volt source to pull up the output of a voltage comparator and to power an inverter logic chip. Four matched 300 Ω and one 11 Ω surface mount resistors are set up in a Wheatstone bridge as shown in the diagram. The leg of the bridge that has only two 300 Ω resistors in series establishes the set point voltage at +7.5 volts. The parallel leg of the bridge, which consists of the two 300 Ω and the one 11 Ω resistors, determines the sensor resistor voltage. The sensor resistor is the 300 Ω resistor connected between ground and the 11 Ω resistor. If the sensor is outside the LN2 bath, the sensor temperature would be close to 300 K due to heat convection and joule heating. In this case, the sensor resistance would be 300 Ω, and the sensor voltage would be 7.36 volts. If the sensor is within the LN2 bath, its temperature would be 77 K, the resistance would be 318 Ω, and the voltage

would be 7.58 volts. In the real circuit, long wire-wrap leads connect the sensor resistor to the rest of the circuit. The leads are long to ensure that the sensor would be able to extend to the cryostat even if the LN2 level detector circuit is located far from the cryostat. Thin wire wrap instead of thicker wires are used for the sensor leads because thicker wires would add extra thermal capacity to the sensor, increasing the time constant of the sensor.
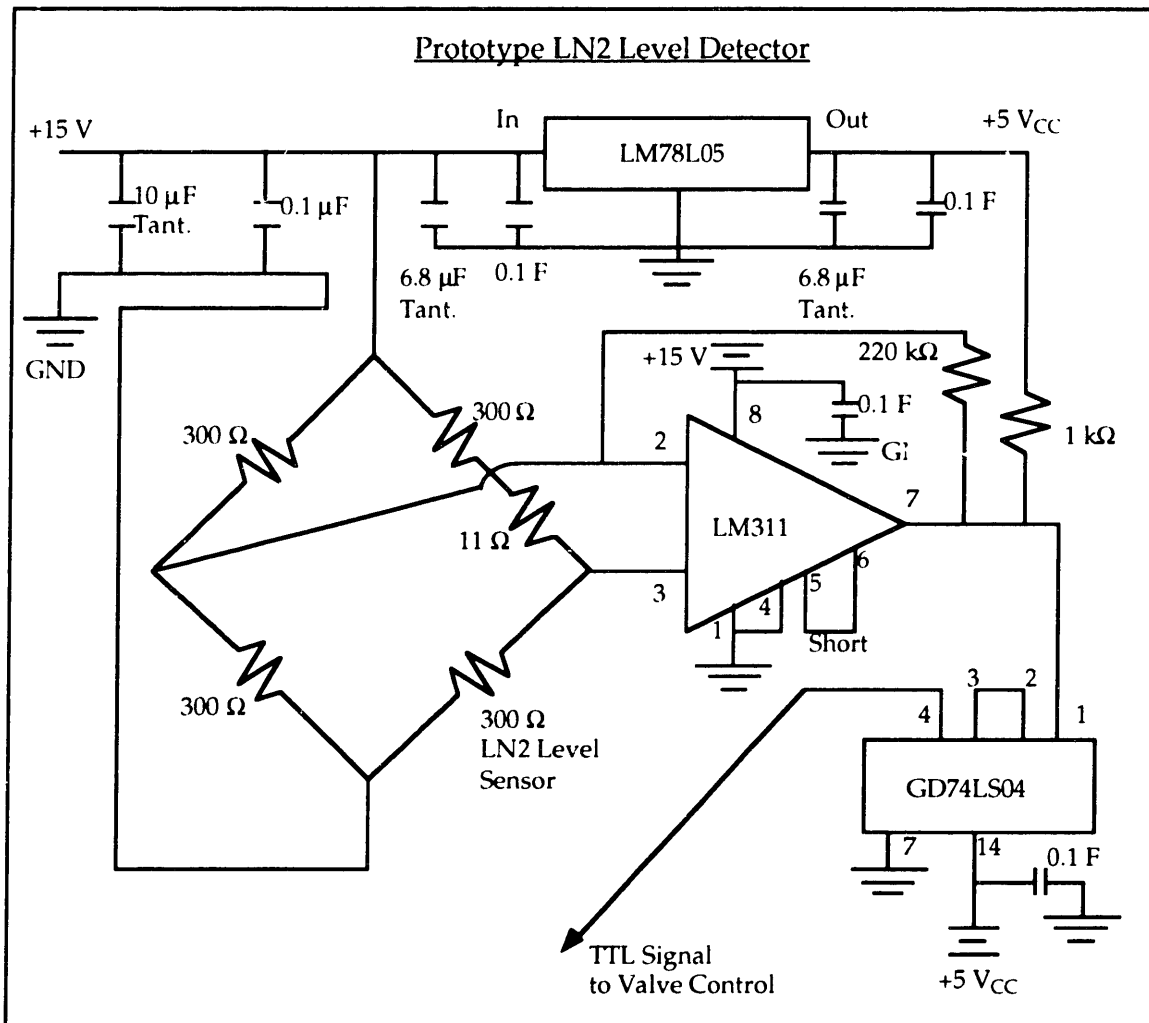

Figure 9: Circuit diagram of the prototype LN2 level detector.

The set point voltage from the bridge is sent to the positive input of an LM311 voltage comparator, and the sensor voltage is sent to the negative input. Positive feedback from the output provides enough hysteresis to attenuate the effects of noise in the input voltages. The comparator output is

29

either 0 volts, if the sensor voltage is less than the reference voltage, or is pulled up to 5 volts, if the sensor voltage is greater than the set point voltage.

The comparator output is sent through two GD74LS04 inverter gates and the resulting TTL signal is sent to the on/off solenoid valve in the LN2 delivery system.

The main issue in designing the LN2 level detector is understanding how the surface mount resistor behaves and adjusting the Wheatstone bridge to take advantage of its resistance characteristics.

4.3.2.   LN2 Pipe Delivery System

The key issues in designing the LN2 pipe delivery system are speed, reliability, and safety. The system must be able to deliver the LN2 to the cryostat quickly to maintain the desired LN2 level and to prevent a magnet quench. The system must operate reliably, delivering the LN2 everytime it is switched on by the level detector. Safety is important because liquid nitrogen is a dangerous substance and must be handled with care.

As shown in Figure 3, the LN2 is provided by a 160 liter dewar with an internal gage pressure of 22 psi. A refrigeration solenoid valve, connected to the exit nozzle of the dewar, is used to open and close the dewar. It is an on/off valve and not a regulator valve. Thus, the flow rate of the LN2 exiting the dewar cannot be controlled.

The other end of the solenoid valve is connected to one foot (0.3 m) of copper pipe extending horizontally, followed by one foot of copper pipe extending vertically. In choosing the appropriate pipe diameter and length, the time delay associated with the LN2 flow through the pipe is considered. The larger the pipe diameter, the longer the time delay. Furthermore, the longer the pipe length, the longer the time delay. For the prototype delivery system, a standard pipe diameter of 3/8 inches is chosen.

Initial tests of the LN2 pipe delivery system show that the LN2 exits the pipe into the cryostat at a high flow velocity. Because the prototype cryostat is only 14.4 cm deep (see Figure 7) and the LN2 level inside is ideally maintained at 11 cm, the exit opening of the pipe is located very close to the LN2 level. Liquid nitrogen rushing into the cryostat at a high velocity creates considerable splashing. This would generate waves at the LN2 surface, causing noise in the sensor voltage signal.

30

To limit excessive LN2 surface wave propagation, the velocity of the LN2 flow from the feed pipe is further reduced by attaching a phase separator, shown in Figure 10, at the pipe exit to create back pressure. A small volume of the slower LN2 evaporates into nitrogen vapor and is vented out through the sides of the phase separator. The rest of the LN2 which has not evaporated gently flows into the cryostat.
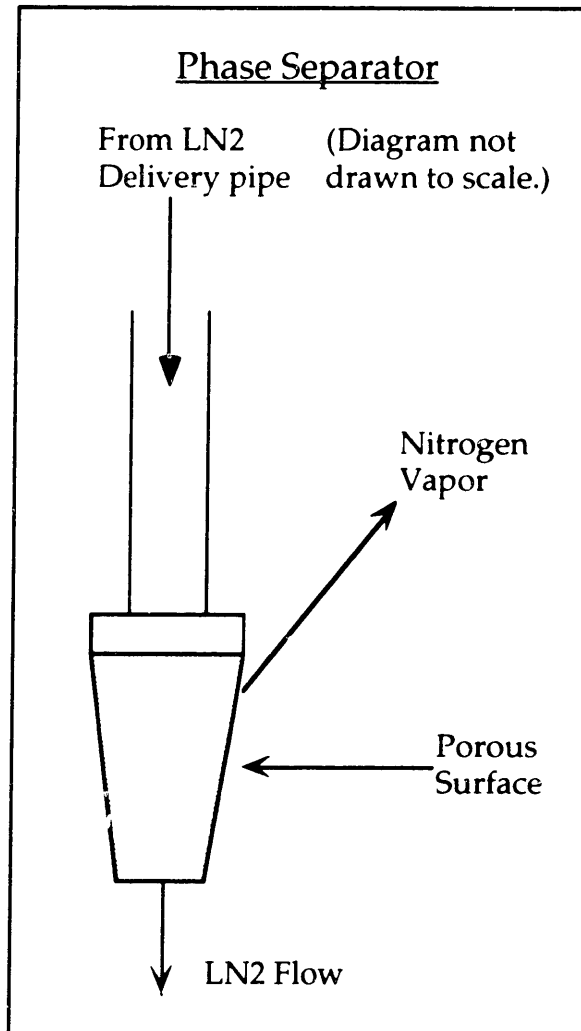
Phase Separator

From LN2
Delivery pipe

(Diagram not
drawn to scale.)

Nitrogen
Vapor

Porous
Surface

LN2 Flow

Figure 10: Phase separator of the prototype LN2 delivery system.

4.3.3. Designing the Mechanical Baffle for the Sensor

Another defense against LN2 surface waves and noisy sensor signals is the use of a mechanical baffle, shown in Figure 11, to house the sensor. The

31

baffle mechanically filters out surface waves and attenuates the in-rush of LN2 into the area of the sensor.

LN2 Level Sensor Mechanical Baffle
(Diagram not drawn to scale.)

Wires to
LN2 Level
Detector
Circuit

Adhesive
Material

1 cm

3.4 cm

Nylon Bolt
(at least 3.5 cm long)

2.4 cm

0.5 cm

LN2 Level
Sensor

2 cm

1 cm

0.076 inch
O.D.
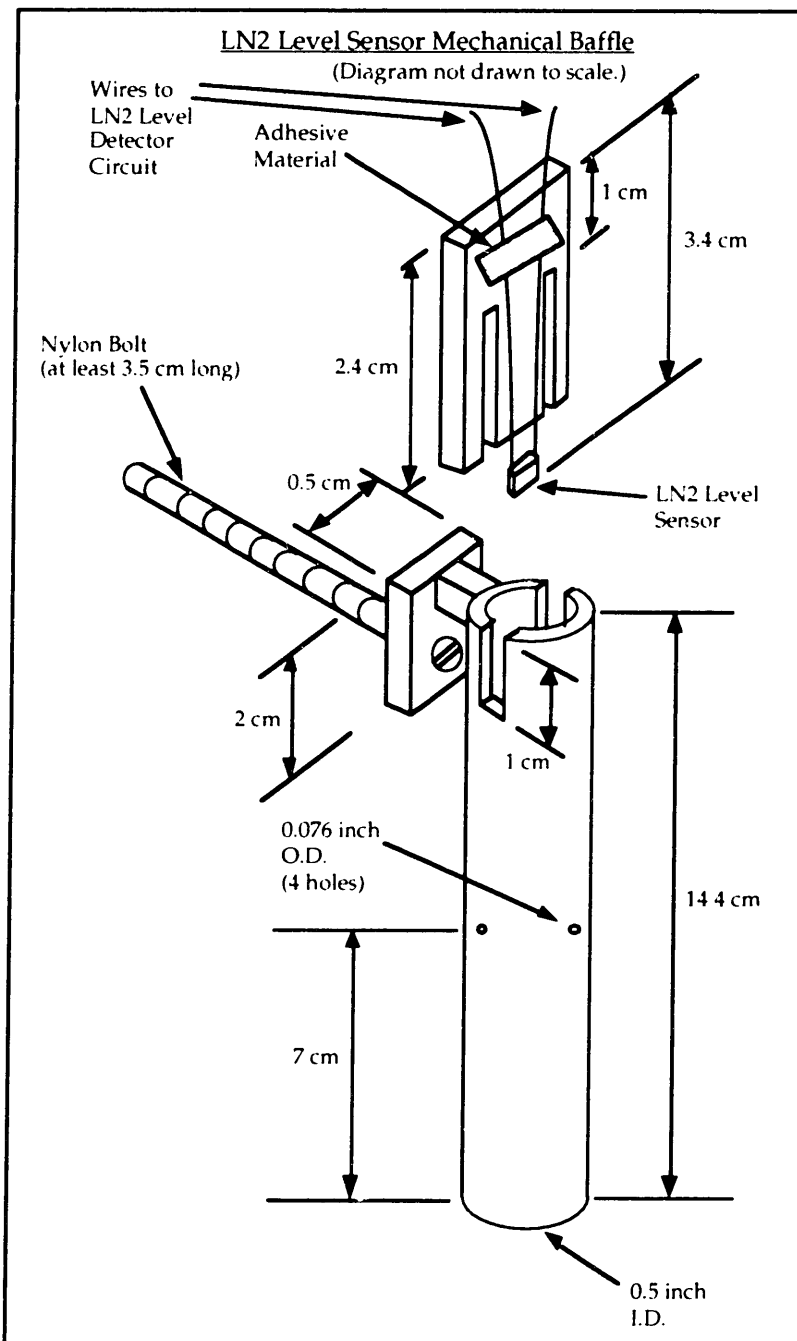(4 holes)

14 4 cm

7 cm

0.5 inch
I.D.

Figure 11: Mechanical baffle for the LN2 level sensor.

The baffle is a 0.5 inch diameter G10 fiberglass tube open at both ends. The level sensor is fixed to a G10 fiberglass insert with a cryogenic adhesive. The insert fits into the tube through the slits. The sensor is suspended at the

desired LN2 height inside the tube so that the sensor does not touch the walls of the tube.[15] The height is adjusted by appropriately fixing the sensor to the insert at the correct location. There are four small holes around the midsection of the tube to allow LN2 to seep into the tube and maintain the LN2 level inside the tube equal with the level outside. The holes are located at the midsection because the LN2 bath should be the calmest at this level.

Finally, the mechanical baffle is bolted to the wall of the cryostat at the diagonal corner from where the LN2 delivery pipe feeds in. This further ensures that any disturbances caused by the LN2 flowing into the cryostat have decayed while propagating across the LN2 bath.

5. Experimental Procedure

Tests were performed on the prototype system to determine the actual LN2 volume flow rate from the delivery system, evaporation rate from the cryostat, and performance of the LN2 level detector and delivery system.

5.1. Measuring the LN2 Volume Flow Rate from Pipe

Before measuring the LN2 volume flow rate from the LN2 delivery system, the cryostat was filled with LN2 in order to bring it to thermal equilibrium with the LN2. A metric ruler was placed vertically within the cryostat and also allowed to cool down to equilibrium with the LN2.

After preparing the cryostat for the test, the LN2 delivery system was switched on. The time it took the LN2 level inside the cryostat to rise by one centimeter was recorded. By knowing the inside horizontal area of the cryostat, the volume flow rate may be calculated.[16]

---

[15]Should the sensor touch the tube wall, the additional heat source from the wall would influence the sensor voltage signal.

[16]Note that the LN2 volume flow rate may be more accurately called the volume fill rate. While LN2 flowed into the cryostat from the delivery system, LN2 in the bath was also evaporating. The difference between these rates was what was actually measured. Because the LN2 volume entering the cryostat was higher than the volume leaving, the level rose.

5.2. Measuring the LN2 Evaporation Rate

Two tests of the LN2 volume evaporation rates were performed. The first test measured the evaporation rate due to heat transfer through the cryostat walls. This test did not have the copper magnet sitting inside the cryostat. The second test measure the evaporation rate due to both heat transfer and joule heating from the copper magnet at full power. From knowing these two rates, the evaporation rate due to only joule heating may be calculated.

To measure the evaporation rate due to heat transfer only, the cryostat was filled with LN2 and left undisturbed. Using a metric ruler, the height of the LN2 level was measured every five minutes and recorded.

Before measuring the evaporation rate due to both heat transfer and joule heating, the cryostat, with the unpowered copper magnet inside, was filled with LN2 until the level was several centimeters ($\approx$ 3 cm) above the top of the magnet. The cryostat and magnet was allowed to reach thermal equilibrium with the LN2 before the magnet was powered with 10 amps. Again, with a metric ruler, the height of the LN2 level was recorded every five minutes.

5.3. Testing the Level Sensor in the Prototype Cryostat

The test of the prototype LN2 delivery system involved measuring the voltage inputs to the comparator of the level detector, and recording the lengths of time the delivery system remained on and off.

With the magnet, LN2 level sensor, and mechanical baffle at a state of thermal equilibrium within an LN2 bath, which was at a level above the height of the sensor at 11 cm, the power to the magnet and level detector was turned on. The set point voltage of the detector bridge was measured with a multimeter. With the sensor within the LN2 bath, the sensor voltage was measured. When the LN2 level evaporated below the sensor, the sensor voltage was measured again.

The prototype system was operated long enough to record several observations of the fill time and evaporation time.

6. Results and Discussion

From tests performed on the prototype system, the actual LN2 flow rate from the delivery system, evaporation rate due to the heat transfer through the cryostat and due to joule heating from the copper magnets, and lengths of time the LN2 delivery system remained on and off were determined. These results were compared with the results of the theoretical analysis and the simulation of the overall prototype system.

6.1. Results from the Flow Rate, Evaporation Rate, and Level Sensor Tests

From measurements made during the flow rate test, the LN2 level in the cryostat rose one centimeter every 68 seconds. Because the prototype cryostat has an internal horizontal cross-sectional area of 307.16 cm^2 (see Figure 7), the LN2 volume of the cryostat increased by 307.16 cm^3 in 68 seconds, leading to a volume flow rate of m'_f = 4.52 cm^3/s.

During the test of the volume evaporation rate only due to heat transfer through the cryostat walls, the LN2 level decreased 0.4 cm every ten minutes. Thus, the LN2 volume decreased 122.86 cm^3 every ten minutes, leading to a volume evaporation rate due to heat transfer of approximately $m'_{e,ht}$ = 0.2 cm^3/s.

The LN2 level decreased 0.8 cm every five minutes during the test of the volume evaporation rate due to both heat transfer through the cryostat walls and joule heating from the copper magnets. Therefore, the LN2 volume decreased 245.73 cm^3 every five minutes, leading to a volume evaporation rate of m'_e = 0.82 cm^3/s.

By knowing $m'_{e,ht}$ and m'_e, the volume evaporation rate due only to joule heating from the magnets was calculated to be $m'_{e,jh}$ = 0.62 cm^3/s.

In the LN2 level detector that was built, the four matched resistors of the Wheatstone bridge were actually 299 Ω each at room temperature, instead of the 300 Ω resistors called for in the design. The 11 Ω resistor in the bridge was measured to be 11.2 Ω at room temperature. Because the voltage source was actually 15.30 volts, the setpoint voltage was measured to be 7.64 volts (instead of the 7.5 volts indicated in the original design). During the test of

35

the LN2 level detector, the sensor voltage swung between 7.54 volts (at a temperature near 300 K since the sensor was suspended in the nitrogen vapors just above the LN2) and 7.72 volts (at 77 K). The original expectation from the design was a swing between 7.36 volts at 300 K and 7.58 volts at 77 K.

During the test of the overall LN2 delivery system, it was observed that the level detector switched the delivery system on and off at a fairly consistent rate. Whenever the LN2 level fell below the sensor, the delivery system remained on and delivered LN2 for 19 seconds. Whenever the LN2 level was above the sensor, the delivery system remained off for 95 seconds.

The results from the various tests done on the overall prototype system are summarized in Table 8.

Table 8:   Results from the LN2 flow rate, evaporation rate, and level detector tests.

LN2 Flow Rate, m'_f	4.52 cm^3/s
LN2 Evaporation Rate from Heat Transfer, $m'_{e,ht}$	0.2 cm^3/s
LN2 Evaporation Rate from Joule Heating, $m'_{e,jh}$	0.62 cm^3/s
LN2 Total Evaporation Rate, m'_e	0.82 cm^3/s
LN2 Delivery System On Time	19 s
LN2 Delivery System Off Time	95 s

6.2.   Discussion of the Experiment Observations

The LN2 volume flow rate, volume evaporation rate, and LN2 delivery system performance were all carefully observed during subsequent tests of the overall prototype system. The tests and observations proved that the overall LN2 delivery system is reliable in maintaining a stable cryogenic environment within the cryostat for the magnet. The LN2 level detector

component of the overall LN2 delivery system performed exceptionally well and as expected.

The LN2 flowed gently into the cryostat from the delivery system during operational tests of the overall prototype system. Because of the low flow rate, no waves or other disturbances of the LN2 bath were created. However, the magnets, powered at 10 amps, produced enough joule heating to cause considerable bubbling in the LN2 bath. This did not seem to affect the LN2 level detector performance, though, as it did not randomly switch the delivery system on and off due to noisy sensor signals. Instead, it consistently switched the delivery system on and off for 19 seconds and 95 seconds, respectively.

It was observed that during the initial portion of the on time (beyond the 0.054 pipe time delay expected), LN2 did not actually flow into the cryostat. It is reasoned that because of the long off time, the delivery pipe system was able to warm up slightly from 77 K. Thus, when the system switched on, LN2 was needed to cool down the pipes again to 77 K. Thus, some LN2 was evaporated in the pipe, and there was a longer delay in delivering the LN2 to the cryostat. However, that delay did not last longer than 2 seconds of the total on time.

From the observations, the overall delivery system was also able to maintain the LN2 level at 11 cm to within ±2 mm. The on and off times of the delivery system supports this observation. Maintaining a flow rate of m'_f = 4.52 cm^3/s for 19 seconds leads to an 85.88 cm^3 increase in the LN2 volume within the cryostat, or a rise of about 3 mm in the LN2 level about the 11 cm mark. Maintaining an evaporation rate of m'_e = 0.82 cm^3/s for 95 seconds leads to a 77.9 cm^3 decrease in the LN2 volume, or a fall of about 3 mm in the LN2 level about the 11 cm mark. Assuming the level sensor was located approximately at the midpoint of the rise and fall of the LN2 level, the height of the LN2 fluctuated by only ±1.5 mm, according to the on/off times.

From Equation 9, and by knowing that the latent heat of vaporization for LN2 is h_L = 161 J/cm^3, the power dissipation associated with each evaporation rate may be calculated. Table 9 shows the three evaporation rates and their corresponding power dissipation.

Table 9: LN2 volume evaporation rates and the corresponding power dissipation.

LN2 Evaporation Rate	Power Dissipation
$m'_{e,ht} = 0.2$ cm^3/s	32.2 W
$m'_{e,jh} = 0.62$ cm^3/s	99.82 W
$m'_e = 0.82$ cm^3/s (total)	132.02 W

6.3. Comparison with the Theoretical Analysis and Simulation

The experimental results and the theoretical results agreed in most areas, except in the LN2 flow rate. Therefore, the initial simulation did not accurately predict the operation of the overall prototype system. Subsequent simulations using parameters based on information and results from the experiments were then performed. Despite the results from the initial simulation, the new simulations indicated that the simulation may model the real prototype to within a fair level of accuracy. Thus, a more comprehensive understanding of the fluid dynamics of the LN2 delivery pipe system will lead to a better theoretical prediction of the overall LN2 delivery system.

The theoretical analysis of the LN2 delivery pipe system showed that the volume flow rate, m'_f, of LN2 would have been 794.28 cm^3/s, whereas the actual flow rate was 4.52 cm^3/s. The difference may be attributed to an incomplete understanding of the exact nature of the pipe system and the various pressure losses across the dewar exit, the on/off valve, and the 90° bend. Furthermore, the theoretical analysis did not take the phase separator into consideration because that was added to the delivery system after the system had been built and initially tested.

A comparison of the actual and theoretical LN2 volume evaporation rate due to both heat transfer and joule heating showed that the analysis is accurate to within 8%. Theoretically, the evaporation rate, m'_e, should be 0.76 cm^3/s. The actual rate was 0.82 cm^3/s. Table 10 shows a comparison of the theoretical and actual power dissipation from the various evaporation rates.

Table 10: Comparison of the theoretical and actual power dissipation from evaporation.

Evaporation Type	Theoretical Power Dissipation	Actual Power Dissipation
Conduction Heat Transfer	32.67 W	32.2 W
Magnet Joule Heating	89 W	99,82 W
Total	121.67 W	132.02 W

The total power dissipation also matched to within 8%. The theoretical power dissipation from the magnet joule heating should be the actual dissipation since each of the two copper magnets have a resistance of 0.445 Ω in 77 K, and were powered at 10 amps. The difference in dissipation values may be due to other sources of power dissipation, such as a variation of coil resistance due to local heating.

The initial simulation (see Figure 5) of the overall prototype system did not predict the actual performance. The simulation showed that the time the delivery system remained on was less than one second, whereas it was 19 seconds in the real system. The simulation also showed that the delivery system remained off for more than 200 seconds, whereas the real system exhibited 95 seconds. The inconsistencies are due to a higher theoretical LN2 flow rate than the actual flow rate. The higher theoretical flow rate caused an overshoot in the level of the LN2 even when the delivery system was turned on for less than one second. This meant that more LN2 would have to evaporate away before the level decreased down to 11 cm again. The initial simulation proves the need for a slower flow rate and perhaps a flow regulator. An overshoot in the LN2 level is undesirable due to the design of the cryostat.

Further simulations of the overall prototype system using the actual flow and evaporation rates, however, showed that the simulation model may accurately predict the prototype performance. Using a flow rate of 4.52 cm^3/s and an evaporation rate of 0.82 cm^3/s in the simulation parameters, the simulation predicted that the delivery system would remain on for about 16 seconds, and remain off for about 79 seconds. These results compared better

to the actual results than the initial simulation results did. The new simulation results also showed that the LN2 level did not deviate from 11 cm by more than ±1.5 mm, which was observed in the experiments. Figure 12 shows the height and flow rate profiles from the new simulations. Figure 13 compares the simulation flow rate with the actual flow rate.

LN2 Flow Rate = 4.52 cm³/s
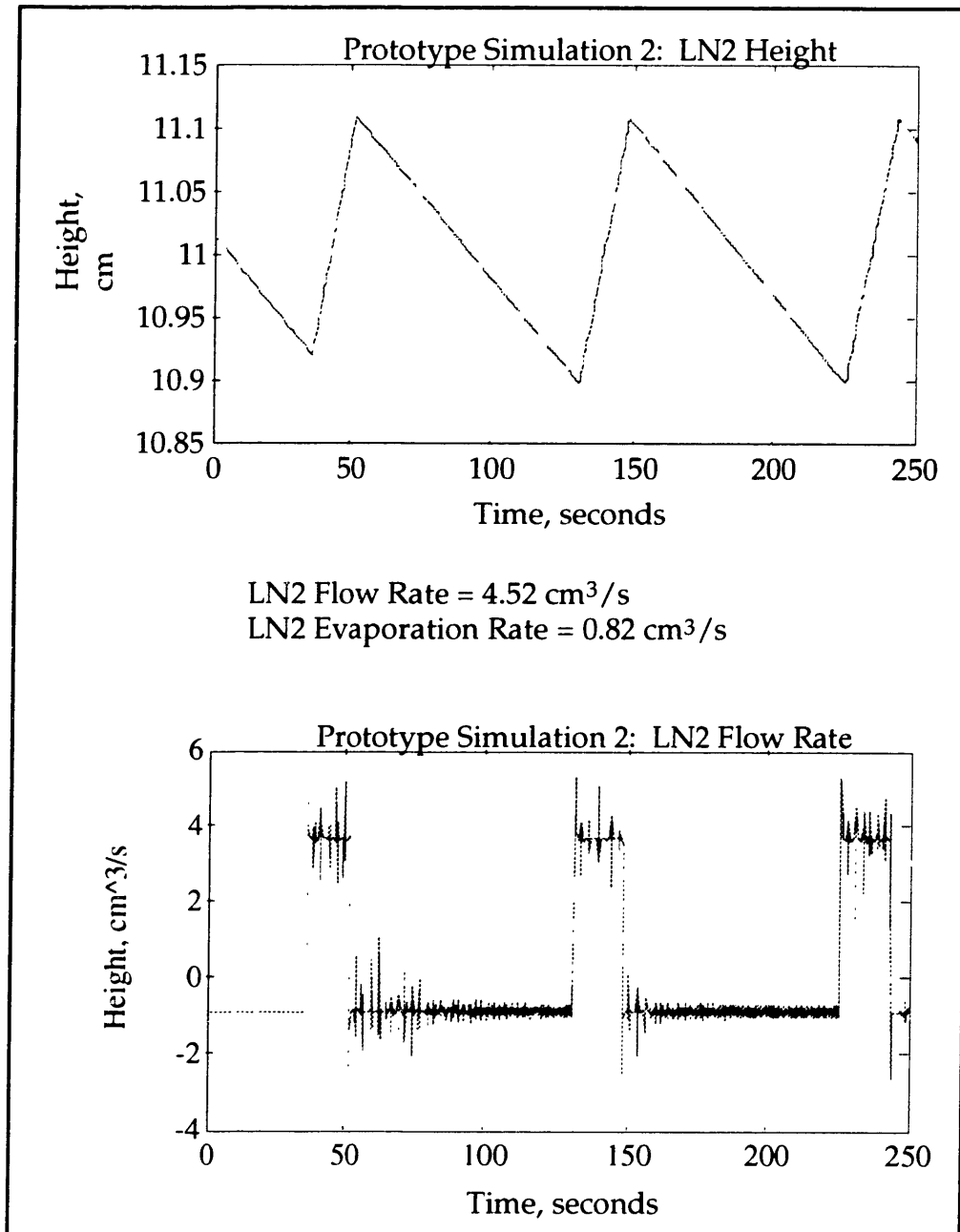LN2 Evaporation Rate = 0.82 cm³/s

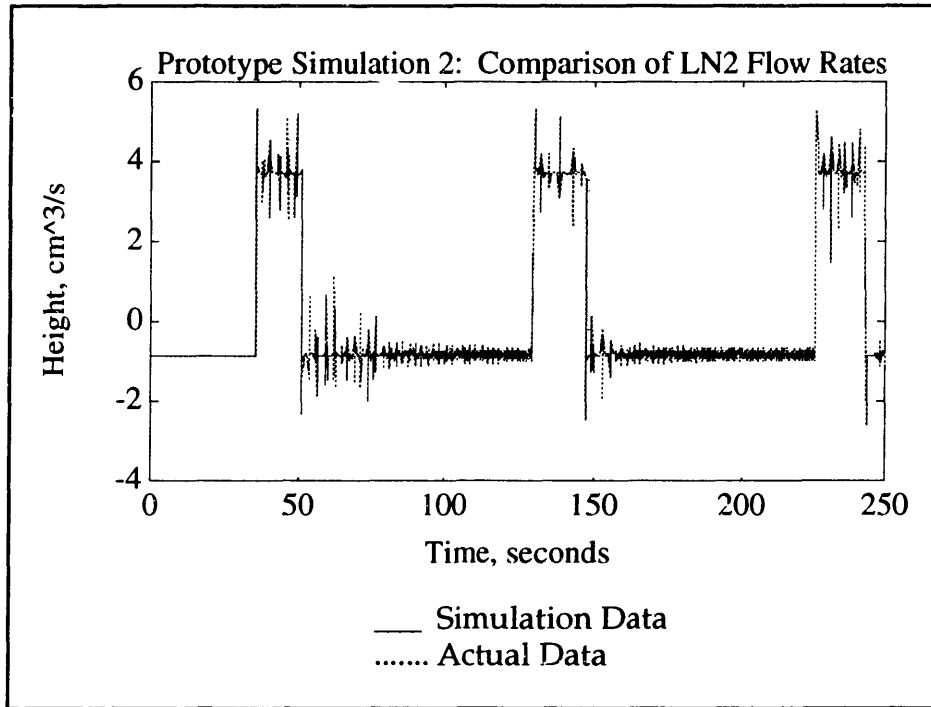Figure 12: Simulation with the actual LN2 flow and evaporation rates from the overall prototype system.

Figure 13: Comparison of the simulation and actual LN2 flow rates for the overall prototype system.

The results from the new simulation indicated that, with a few improvements in the theoretical understanding of the fluid dynamics of the delivery pipe system, the theoretical analysis and simulation model may be used to predict the overall prototype system performance. This also showed that it is possible to adapt the prototype analysis and simulation to a full scale LN2 delivery, cryostat and magnet system.

7. Conclusions and Recommendations

The agreement between the experimental results and the new simulation results discussed in Section 6.3 shows that the theoretical analysis and simulation model for the prototype system may be used as the basis of an analysis and simulation model for a full scale system. However, it is recognized that improvements in the prototype analysis and simulation is needed to achieve better prediction accuracy for the prototype system and, subsequently, for the full scale system. Therefore, suggestions for further research are discussed at the end of this section.

41

7.1. Scaling Up to the Full Scale System

Work is currently being done at the MIT Laboratory for Electromagnetic and Electronic Systems (LEES) and at Draper Laboratory to construct and test a scale-model, high-temperature superconducting magnet design for MAGLEV applications. The magnet will be operated as part of a MAGLEV rotating wheel test facility in Draper Laboratory [6, pp. 6].

Because the prototype system studied in this project (the prototype LN2 delivery system, prototype cryostat, and prototype magnet) is actually a smaller scale model of the system described above, the above system is referred to as the full scale system (relative to the prototype system) in this report.

The full scale system, like the prototype, also consists of an LN2 delivery system, cryostat, and magnet. The cryostat, shown in Figure 14, is simply a larger version of the prototype cryostat, with a few differences in design. The magnet will be an iron core magnet with eight copper coils in series. This full scale copper magnet is used to model the high-temperature superconducting magnet that will be built and tested later.

Again, the goal is to design and analyze an LN2 delivery system, based on the prototype, for the full scale system.
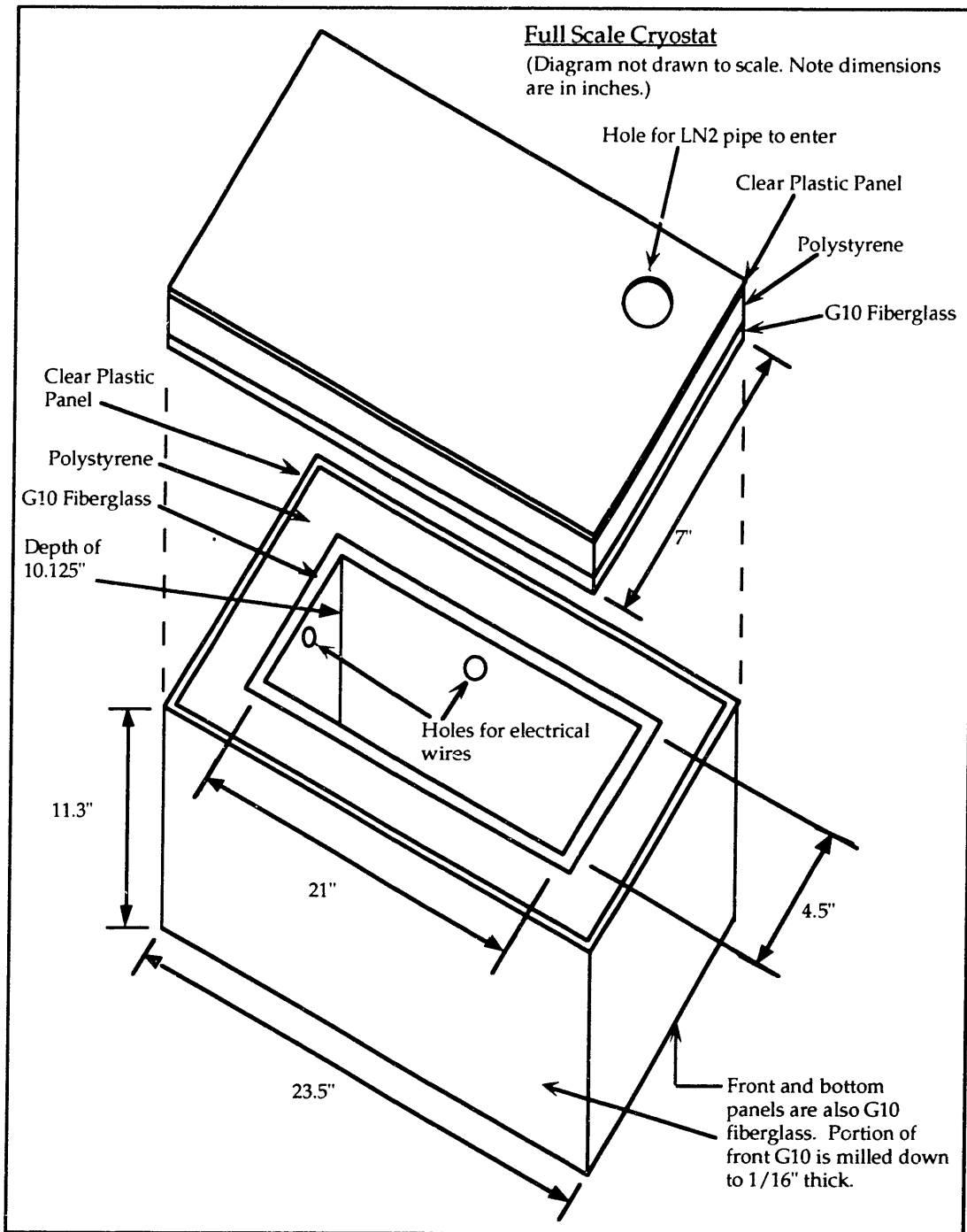
Figure 14: Full scale cryostat.

7.1.1. Analysis of the Full Scale LN2 Evaporation Rate

The LN2 volume evaporation rate for the full scale system is depends on the power dissipation due to joule heating from the eight copper magnets and

conduction heat transfer through the cryostat walls. Radiation heat transfer from the surfaces inside the cryostat is again ignored based upon the reasoning presented in Section 2.2.2.

The convection heat transfer for the full scale cryostat is considerably more complicated than that for the prototype. The prototype cryostat was operated in ambient air at a room temperature of 300 K. The full scale cryostat, on the other hand, will be operated in a vertical MAGLEV rotating wheel test facility. The front face of the cryostat will be located one centimeter from the perimeter of the vertical wheel. The two-meter-diameter wheel will be rotating with a maximum speed of 1000 rpm, which corresponds to a tangential velocity of 100 m/s [6, pp. 19]. These conditions greatly affect the convection heat transfer between the front face of the cryostat and the air in the one centimeter gap. Again, because an analysis of this convective heat transfer is beyond the scope of this study, it will also be ignored in calculating the evaporation rate. Since convection tends to lower the surface temperature of the front face of the cryostat, it may be reasonable to assume that the upper limit of the heat transfer through the cryostat walls is determined by neglecting thermal convection and assuming a surface temperature of 300 K on all six faces. A more detailed discussion of convective heat transfer may be found in Section 2.2.2.

The copper coil magnets in the full scale system are the same as the ones in the prototype system. Thus, each coil will have an electrical resistance of R = 0.445 Ω. Each of the eight coils will be operated with at most 15 amps. Thus, from Equation 1, the total power dissipation from the eight copper coil magnets is expected to be P_E = 801 watts. This is the joule heating portion of the total power dissipation.

Because of certain design changes in the walls of the full scale cryostat, calculation of the conduction heat transfer power dissipation is slightly more involved compared to that for the prototype cryostat. A portion of the 1/8 inch thick front face of the full scale cryostat is milled down to 1/16 inches and does not have a layer polystyrene insulation panel. There is also an aluminum base plate, embedded in the polystyrene panel on the bottom face of the cryostat, to which the full scale magnet is bolted in place. The details of the conduction heat transfer analysis may be found in Appendix **8.3**. Only the results are presented here.

44

The power dissipation due to conduction heat transfer through the full scale cryostat is calculated to be P_C = 6250.95 watts. The total power dissipation in the cryostat, due to both joule heating from the magnet and conduction heat transfer, is P_T = P_E + P_C = 7051.95 watts. From Equation 9, the corresponding LN2 volume evaporation rate for the full scale system is m'_E = 43.80 cm^3/s. The results are listed in Table 11.

Table 11: Full scale power dissipation and LN2 volume evaporation rate.

Magnet Power Dissipation, P_E	801 W
Conduction Power Dissipation, P_C	6250.95 W
Total Power Dissipation, P_T	7051.95 W
LN2 Volume Evaporation Rate, m'_E	43.80 cm^3/s

7.1.2. Analysis of the Full Scale LN2 Flow Rate and Pipe Time Delay

The analysis of the full scale LN2 volume flow rate from the delivery system follows that for the prototype system. The same LN2 delivery system designed for the prototype cryostat will be used for the full scale cryostat (see Figure 3). The only difference is that the full scale version of the delivery system has two meters of copper pipe extending horizontally from the on/off valve exit, and two meters of copper pipe extending vertically from the end of the horizontal pipe. The longer pipes are need to reach over and down into the pit in which the full scale cryostat and wheel are located.

The parameters used in solving for the LN2 velocity exiting the delivery system, listed in Table 5, may be used again in Equation 14 to solve for the full scale exit velocity, V_2. The only difference is that the term (z_1 - z_2) is now 2 meters because of the extra length of vertical pipe. The LN2 velocity exiting the dewar, V_1, is still 19 m/s. The resulting LN2 exit velocity is thus calculated to be V_2 = 11.63 m/s. Note that this velocity, as in the prototype calculation, does not take the effects of the phase separator into account.

With a pipe cross-sectional area of A = 7.13×10^{-5} m^2 (pipe diameter of 3/8 inch), the corresponding full scale LN2 volume flow rate is m'_F = 829.22 cm^3/s. With a total pipe length of four meters, the time delay for the delivery system is T_D = 0.344 s. These results are summarized in Table 12.

Table 12: Full scale LN2 volume flow rate and delivery system time delay.

Delivery System Exit Velocity, V_2	11.63 m/s
Pipe Area, A	7.13×10^{-5} m^2 (3/8 inch inner diameter)
Total Pipe Length, l	4 m
LN2 Volume Flow Rate, m'_F	829.22 cm^3/s
Delivery System Time Delay, T_D	0.344 s

7.1.3. Simulation Results

Because the Simulink block diagram model used in simulating the prototype system seems to characterize the prototype performance fairly accurately in the second simulation, the model is also used to predict the performance of the full scale system.

Table 13 lists the parameters used for the initial simulation of the full scale system. Note that the LN2 volume flow rate is very high. As seen in the initial simulation of the prototype system, the high flow rate is expected to cause an overshoot in the LN2 level.

Table 13: Parameters for the initial simulation of the full scale system.

Parameter	Value
LN2 Volume Flow Rate, m'_F	829.22 cm^3/s
LN2 Volume Evaporation Rate, m'_E	43.80 cm^3/s
LN2 Height, h	22 cm
Pipe Delay, T_D	0.344 s

On/Off Valve Time Constant, τ_v	0.1 s
LN2 Level Detector Time Constant, τ_s	0.31 s
Ideal LN2 Bath Volume, v_b	13,412.88 cm^3
Box Fill Constant (1/Area)	1.64x10^{-3} m^{-2}

Figure 15 shows the LN2 height and flow rate profiles for the initial, 250 second simulation of the full scale system. The graphs only show the first 50 seconds of the simulation. As expected, the high flow rate caused an overshoot in the LN2 level.

A slower LN2 flow rate is needed to eliminate the overshoot in the LN2 level. Again, it is desired to maintain the LN2 level, 22 cm for the full scale system (2 cm above the top of the magnet), to within ±1 mm. In the prototype system, the real flow rate was larger than the real evaporation rate by a factor of 5.5. Thus, for the second full scale simulation, an LN2 volume flow rate of m'_F = 241.43 cm^3/s, which is 5.5 times greater than the expected evaporation rate of m'_E = 43.80 cm^3/s, was attempted.
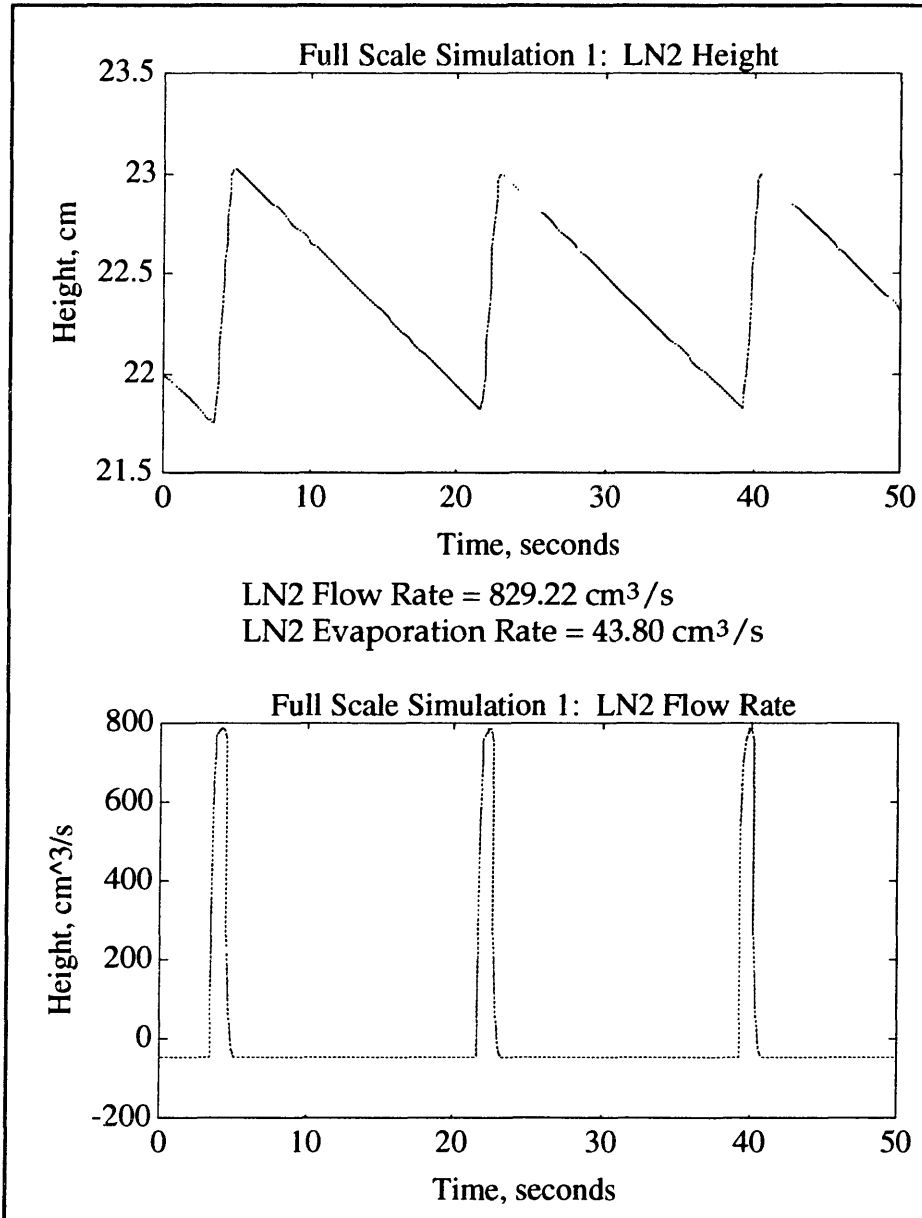
Figure 15: Initial simulation of the full scale system.

Figure 16 shows the LN2 height and flow rate profiles for this simulation. The graphs show that the new flow rate is still not low enough. There is still an overshoot in the LN2 level.

Another method to ensure that the LN2 level does not overshoot is to select an LN2 flow rate that is not much higher than the evaporation rate. The expectation is that the level will rise slowly as just slightly less LN2 evaporates out of the cryostat than flows in. Thus, for the third simulation of

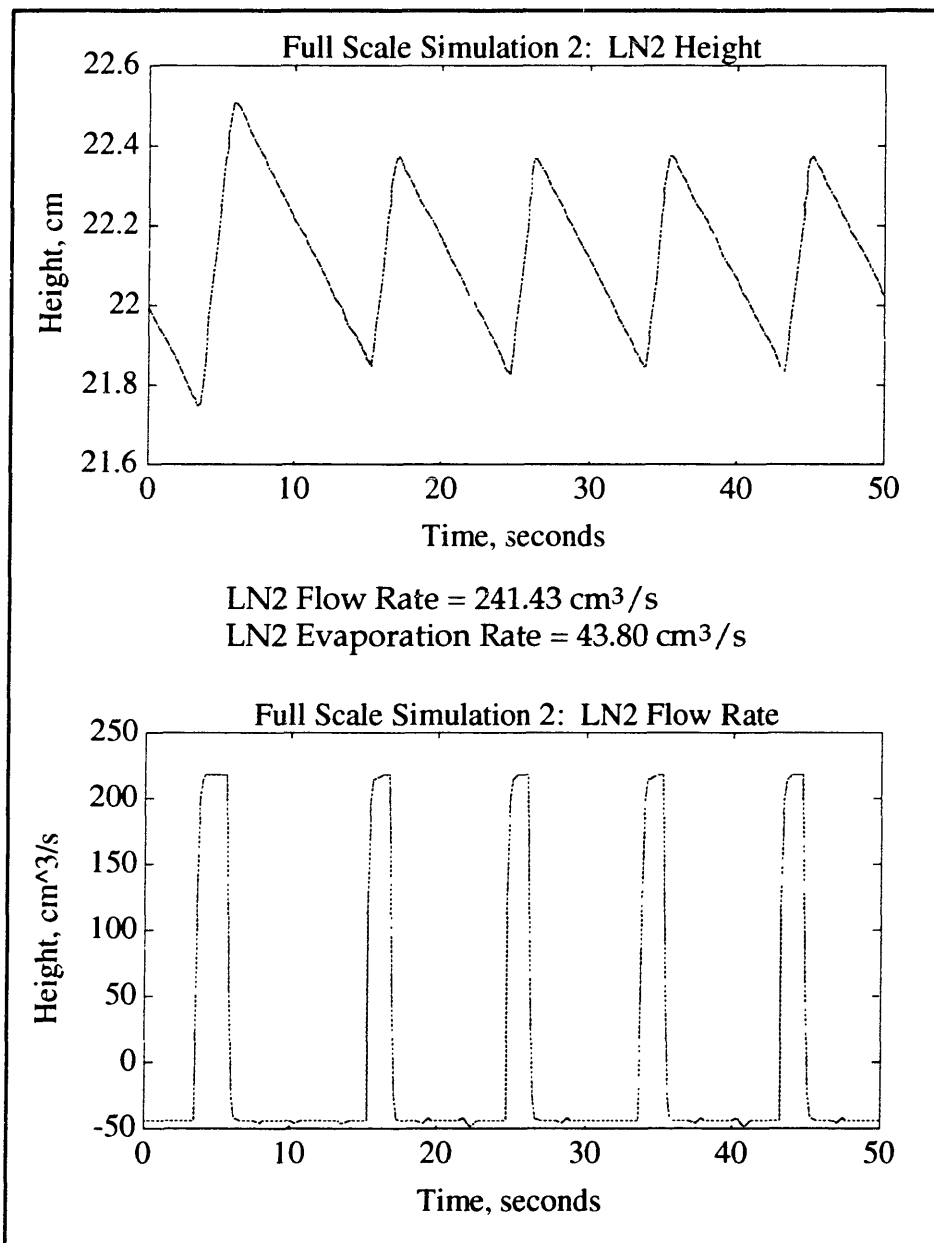the full scale system, a flow rate that is only 20% higher than the evaporation rate was selected.

Figure 16: Full scale simulation with an LN2 flow rate of $m'_F = 241.43$ cm³/s.

Figure 17 shows the LN2 height and flow rate profiles for the third simulation using the new flow rate of $m'_F = 52.56$ cm³/s. These graphs show that the LN2 level does not overshoot. Rather, the level fluctuates about the 22 cm mark to within ±3 mm. The LN2 delivery system remains on for about 20 seconds, and remains off for about 4 seconds.
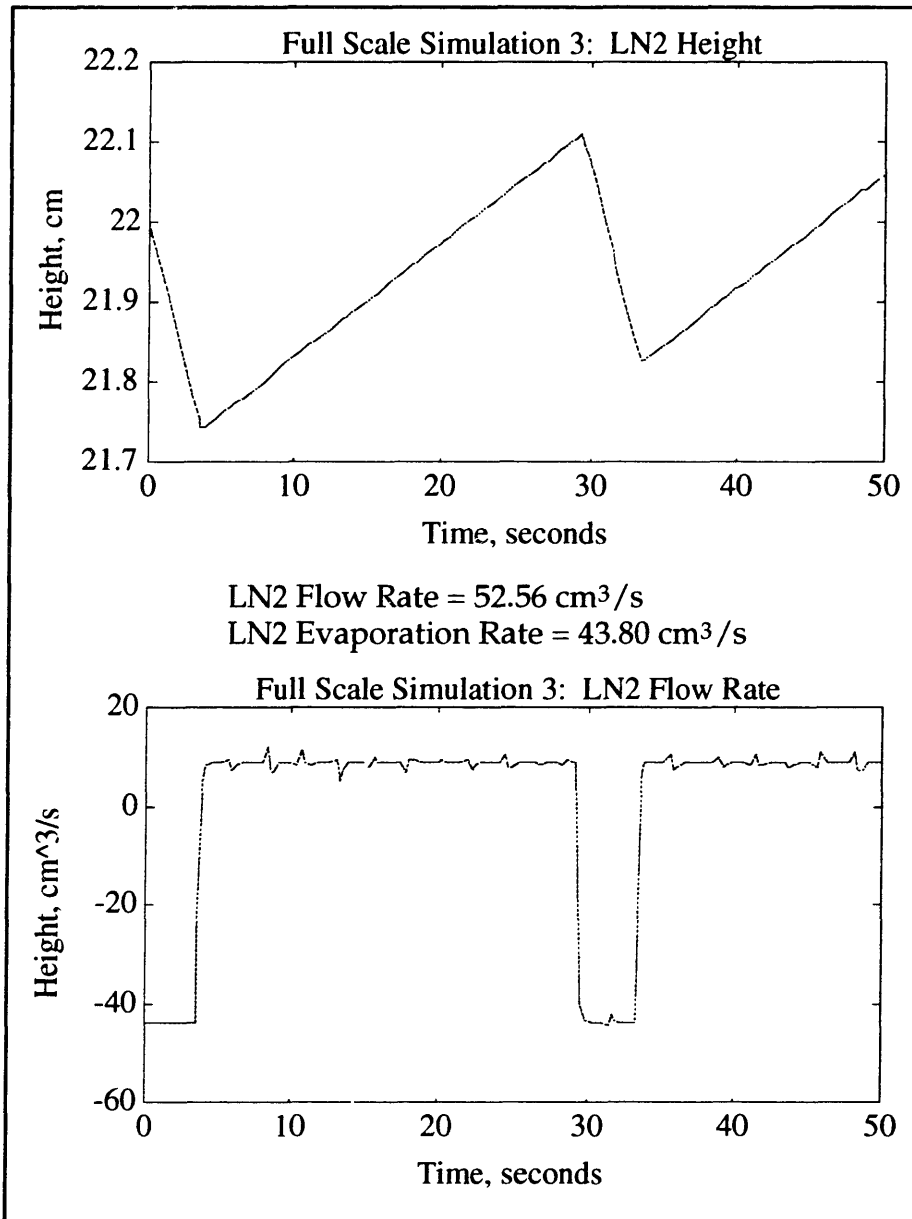
Figure 17: Full scale simulation using a flow rate of $m'_F = 52.56$ cm^3/s.

This full scale simulation indicates that the LN2 delivery system, operating with an LN2 flow rate of $m'_F = 52.56$ cm^3/s, is capable of maintaining the desired level of 22 cm in the full scale cryostat to within a small tolerance. There exists another advantage to using a flow rate that is 20% higher than the evaporation rate. As the simulation shows, the LN2 delivery system remained on for about 20 seconds, and remained off for only 4 seconds. Observations of the prototype system reveals that a long off time allows the delivery pipe system time to warm up from 77 K. Consequently, the initial

portion of the on time is spent cooling the pipe system back down to 77 K, evaporating the lead volume of flowing LN2. Thus, the actual pipe delay must take the time to cool the pipes into consideration with the time for the LN2 to flow from beginning to end. With a longer on time and shorter off time, as in the full scale simulation, the delivery system has less time to warm, less LN2 is evaporated in cooling the pipes back to 77 K, and the pipe time delay becomes more dependent on the pipe dimensions (length) and less dependent on pipe cooling time.

As the simulations show, a full scale LN2 delivery system based on the prototype LN2 level detector and delivery system may perform reliably. The performance of a full scale LN2 delivery system depends on choosing a low LN2 volume flow rate. As the full scale simulations show, a flow rate that is only 20% higher than the evaporation rate will maintain a steady LN2 height to within a few millimeters. The tolerance may be further reduced by lowering the flow rate.

7.2. Avenues for Further Research

The successful performance of the prototype LN2 delivery system encourages the development of a full scale version based upon the prototype. Because the simulation model was able to predict the performance of the prototype, it will be used in the design of the full scale system. The observations and results from the prototype system and simulation provide enough information for a successful design.

Of course, further research is suggested to improve upon the results of this study. As the initial prototype simulation showed, a more comprehensive understanding of the fluid dynamics of the LN2 delivery pipe system is needed. The theoretical analysis of the pipe system presented in this study dealt with an idealized model of the system. Thus, by examining the pipe system more carefully, a model that closely resembles the actual system may be developed for the theoretical analysis. This will lead to better predictions of the LN2 volume flow rate and pipe time delay.

The idealization of the heat transfer analysis for the cryostat to just an analysis of the thermal conduction process and joule heating provided a fairly accurate prediction of the power dissipation and LN2 evaporation rate for the

prototype system. That provides support for the results of the full scale heat transfer analysis. Of course, it is reasonable to assume that thermal convection and other heat transfer processes do affect the power dissipation analysis. However, the extent of those effects are not understood. Further study into the heat transfer associated with the cryostat may lead to more accurate predictions of the power dissipation to the LN2 bath and of the LN2 volume evaporation rate.

Another area for further study is the design of the LN2 level detector. Other methods for sensing the LN2 level, such as using bimetallic strips or photodiodes, may be investigated. The main considerations in these investigations should be improving sensing tolerance and maintaining detector reliability.

Finally, methods for decreasing the pipe time delay may be studied. A few suggestions include studying the effects of including a bias flow in the pipe system, insulating the pipe system so that the pipes do not warm up as fast during off times, and optimization of the LN2 flow velocity and volume flow rate.

8. Appendices

8.1. Simulink Block System Simulation

The Simulink block diagram model of the prototype and full scale systems is explain in more detail here. For convenience, the block diagram shown in Figure 4 is reproduced in Figure 18.

The On/Off Valve block is a hysteretic component that controls the LN2 volume flow. Whenever its input is +0.1 or more, the LN2 level is higher than 0.1 cm above the desired height, and the flow is turned off (0 cm^3/s). When the input is -0.1, the LN2 level is lower than 0.1 cm below the desired height, and the flow turns on to whatever value it is given.

The Valve Time Constant component represents the transfer function of the valve. A valve time constant of 0.1 seconds is assumed for the solenoid valve because it was observed to be very fast. It was not actually measured. The accuracy of some of the simulations indicated that this was a reasonable assumption.
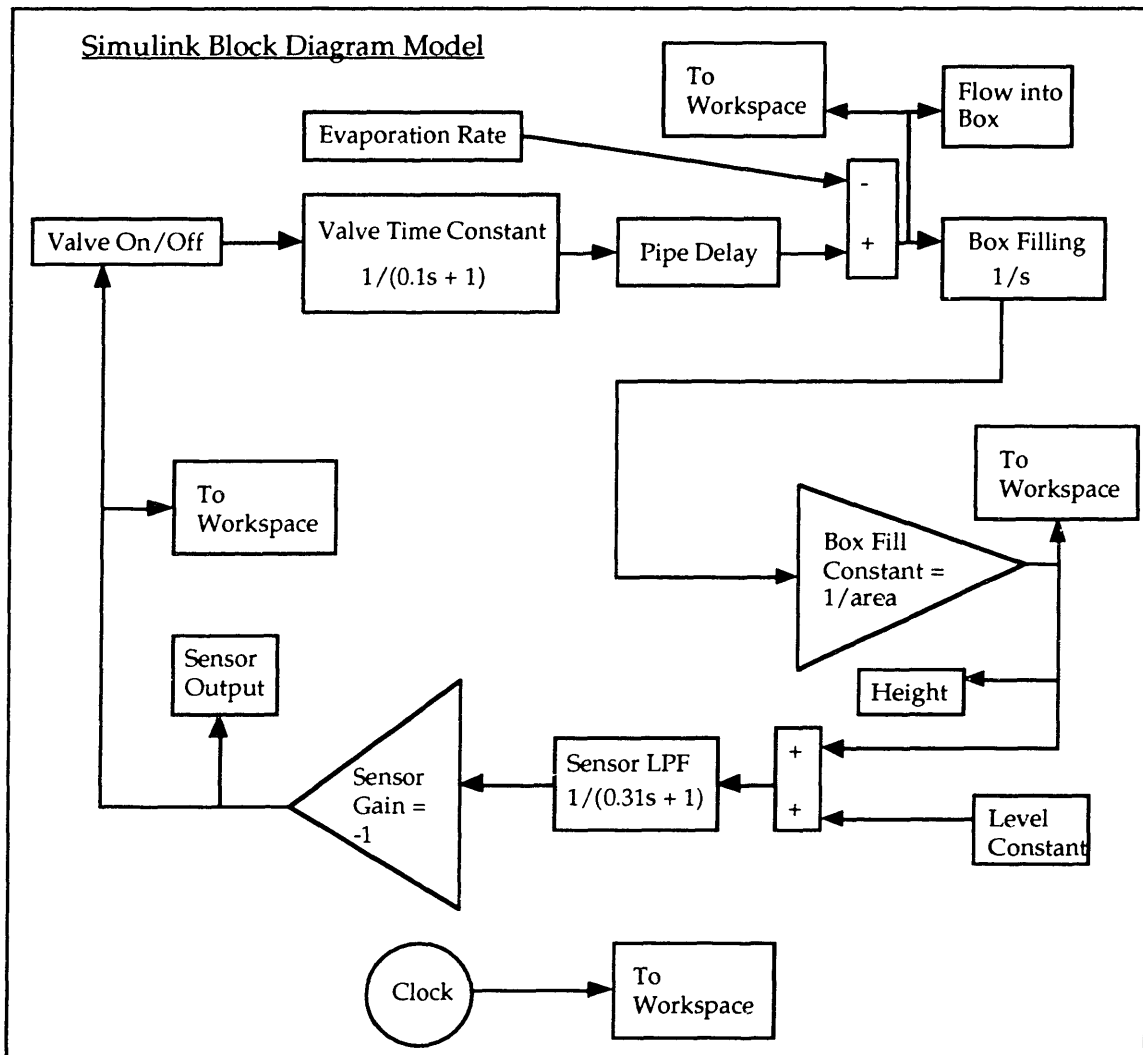
Figure 18: Simulink block diagram model of the prototype and full scale systems.

The Pipe Delay component represents how long it takes the LN2 to flow through the pipe. It is based on the flow velocity and the pipe length.

The Evaporation component represents the evaporation rate, and is a constant input to the Summation component.

The Summation component accepts the flow rate and the evaporation rate as inputs, and send the result to the Box Filling component.

The Box Filling component integrates the input and outputs the total volume of LN2 inside the cryostat. An initial LN2 volume input is entered into this component as a starting point.

The Box Fill Constant component multiplies the volume input by a constant, the inverse of the horizontal cross-sectional area of the cryostat. The output is the current LN2 height in the cryostat.

Another Summation component takes the current LN2 height input and subtracts the ideal height from it. The difference is sent to the Sensor Low Pass Filter (LPF) component, which represents the transfer function of the LN2 level detector. The time constant of 0.31 seconds was calculated from observations of the real detector. It was also not measured. The accuracy of a few of the simulations indicates that this is a reasonable assumption for the sensor time constant.

The Sensor Gain component inverts the input from the Sensor LPF component, and sends it to the ON/Off Valve component.

The Height, Flow into Box, and Sensor Output components produces a plot of the variables versus time. The To Workspace components sends the data to a buffer in memory.

8.2. Resistor Test and Data

In selecting the appropriate resistor to use as the LN2 level sensor, the temperature dependent resistance variation of each type of resistor tested is examined. The test for the resistance variation consisted of simply dipping each resistor in an LN2 bath and measuring the final resistance with an ohm meter. Table 14 lists the results of the tests on the resistors. Those resistors with an asterisks * next to them are the ones used in the LN2 level detector. Carbon composition resistors are indicated by CC, and surface mount resistors are indicated by SM.

Table 14: Results of the resistor tests.

Resistor Type	Ω at 300 K	Ω at 77 K	Time to Change Resistance, sec.
CC 100 Ω	107.2	132	3
CC 1.8 k Ω	1.86 k	2.61 k	3
SM 100 Ω	100	107.3	3
SM 820 Ω	839	875	3
SM 300 Ω	297	313	1

SM 300 Ω	298	315	1
SM 300 Ω *	298	317	1
SM 300 Ω *	299	318	1
SM 300 Ω *	299	317	1
SM 300 Ω *	298	317	1
SM 300 Ω	298	315	1
SM 11 Ω	11.3	11.97	1
SM 11 Ω *	11.2	11.95	1
SM 11 Ω	11.2	11.88	1

8.3. Conduction Heat Transfer Analysis for the Full Scale Cryostat

The heat conduction through the walls of the full scale cryostat is not the same as that of the prototype cryostat because the design of the front and bottom walls of the full scale cryostat differs from those of the prototype. Refer to Figure 14 for the dimensions of the full scale cryostat.

The outside panel of the full scale cryostat is 1/8 inch thick G10 fiberglass instead of the clear plastic panel. A large portion of this G10 panel is milled down to a thickness of 1/16 inches. The full scale magnet is located on the inside of this milled down portion of G10. There is no polystyrene insulation along the inside of the milled down portion of G10, and the inner panel of G10 is not present. The rest of the outside G10 panel is still 1/8 inch thick, and a polystyrene panel and another G10 panel lie to the inside of the outside panel. Figure 19 shows the cross sections of the front wall through the milled down portion and the unmilled portion.

The power dissipation, or heat transfer rate, through the milled down portion of G10 may be determined by applying directly Equation 3 and Equation 4. The area of the milled down portion is A_m = 774.17 cm². Thus, the power dissipation, P_1, through this portion is:

$$P_1 = k_G A_m \frac{T_1 - T_2}{L_G} = (0.56) (774.14 \times 10^{-4}) \frac{(300 - 77)}{1.59 \times 10^{-3}}$$
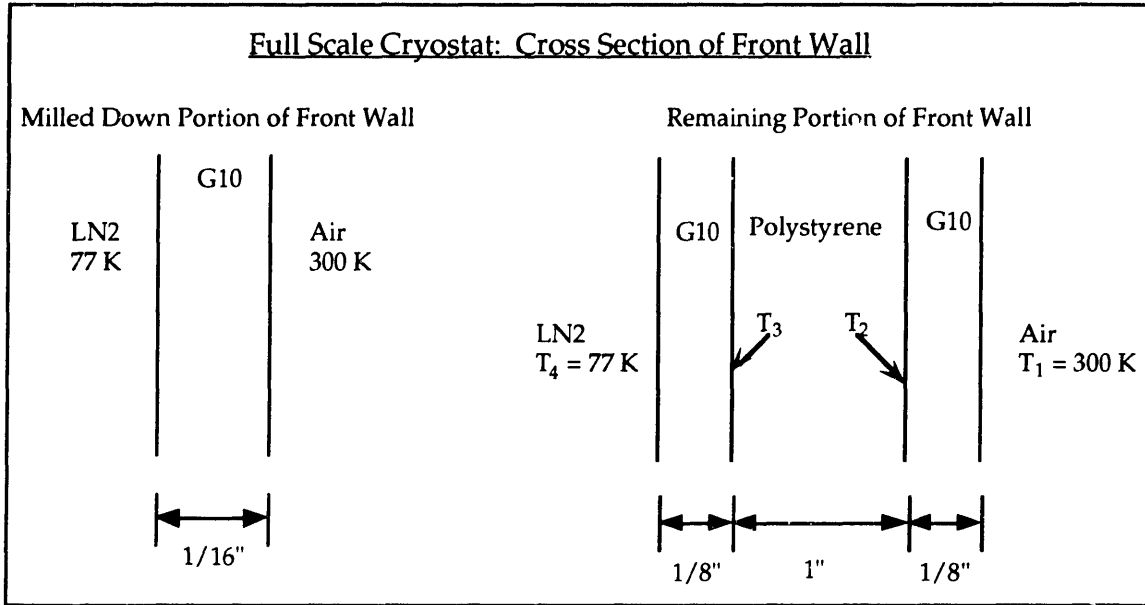
$$P_1 = 6080.40 \text{ watts}$$

Figure 19: Cross sections of the full scale cryostat front wall.

The power dissipation, P_2, through the rest of the front wall may be determined by first solving for the interface temperatures, T_2 and T_3. The temperatures may be determined by applying Equation 3 to each material, equating the heat flux through the outside G10 panel with the heat flux through the polystyrene, solving for T_2 in terms of T_3, equating the heat flux through the polystyrene with the heat flux through the inside G10 panel, substituting the expression for T_2 into that equation, and solving for T_3 in the final equation. The final expressions for T_2 and T_3 are:

$$T_2 = \frac{\frac{k_G}{L_G} T_1 + \frac{k_P}{L_P} T_3}{\frac{k_P}{L_P} + \frac{k_G}{L_G}} \tag{15}$$

$$T_3 = \frac{\frac{k_P}{L_P}\left(\frac{\frac{k_G}{L_G} T_1}{\frac{k_P}{L_P} + \frac{k_G}{L_G}}\right) + \frac{k_G}{L_G} T_4}{\frac{k_G}{L_G} + \frac{k_P}{L_P} - \frac{k_P}{L_P}\left(\frac{\frac{k_P}{L_P}}{\frac{k_P}{L_P} + \frac{k_G}{L_G}}\right)} \tag{16}$$

The interface temperatures are determined to be $T_2 = 298.91$ K and $T_3 = 78.09$ K. Applying Equation 3 and Equation 4 to any one of these panels will then determine the power dissipation, P_2, through the unmilled portion of the

56

front wall. The area of the unmilled portion is A_u = 597.73 cm^2, and the power dissipation is:

$$P_2 = 11.49 \text{ watts}$$

The bottom wall of the full scale cryostat has an aluminum plate embedded within the polystyrene panel. The full scale magnet is bolted to this plate through the bottom wall. The plate has horizontal dimensions of 20.32 cm (8 inches) by 10.16 cm (4 inches), giving it a horizontal cross-sectional area of A_a = 2.06x10^{-2} m^2, and has a thickness of 0.635 cm (1/4 inches). Figure 20 shows the cross sections of the bottom wall through the portion with the aluminum plate and through the portion without.
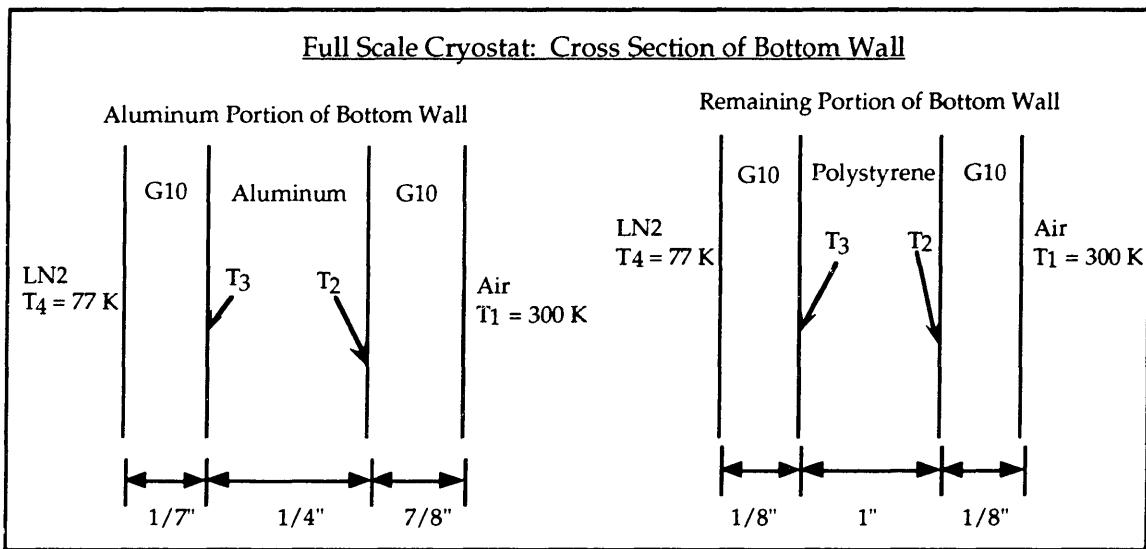

Figure 20: Cross sections of the bottom wall of the full scale cryostat.

To determine the power dissipation through the portion with the aluminum plate, the interface temperatures, T_2 and T_3, must first be solved. The analysis is the same as that for the unmilled portion of the front wall. Thus, Equation 15 and Equation 16 are the same expressions derived for T_2 and T_3, respectively, for the bottom wall. The only difference is that the thermal conductivity [4, pp. 12-119] and thickness for aluminum, K_A = 237 W/mK and L_A = 6.35x10^{-3} m, replaces those for polystyrene in the equations. The temperatures are determined to be T_2 = 105.02 K and T_3 = 104.89 K. Again, after applying the appropriate equations to any layer, the power dissipation, P_3, through the portion of the bottom wall with the aluminum plate is:

$$P_3 = 101.32 \text{ watts}$$

In solving for the power dissipation through the rest of the bottom wall, the temperature equations are used again to solve for T_2 and T_3. Since the cross section of the remaining portion of the bottom wall is the same as that of the remaining portion of the front wall, the interface temperatures are the same, $T_2 = 298.91$ K and $T_3 = 78.09$ K. The area of the remaining portion of the bottom wall is $A_r = 4.04 \times 10^{-2}$ m^2, and the power dissipation, P_4, is:

$$P_4 = 7.77 \text{ watts}$$

The analysis of the power dissipation through the two side walls, the rear wall and the top wall follows the same analysis for the walls of the prototype cryostat. Figure 21 shows the cross section of the remaining four walls of the full scale cryostat.
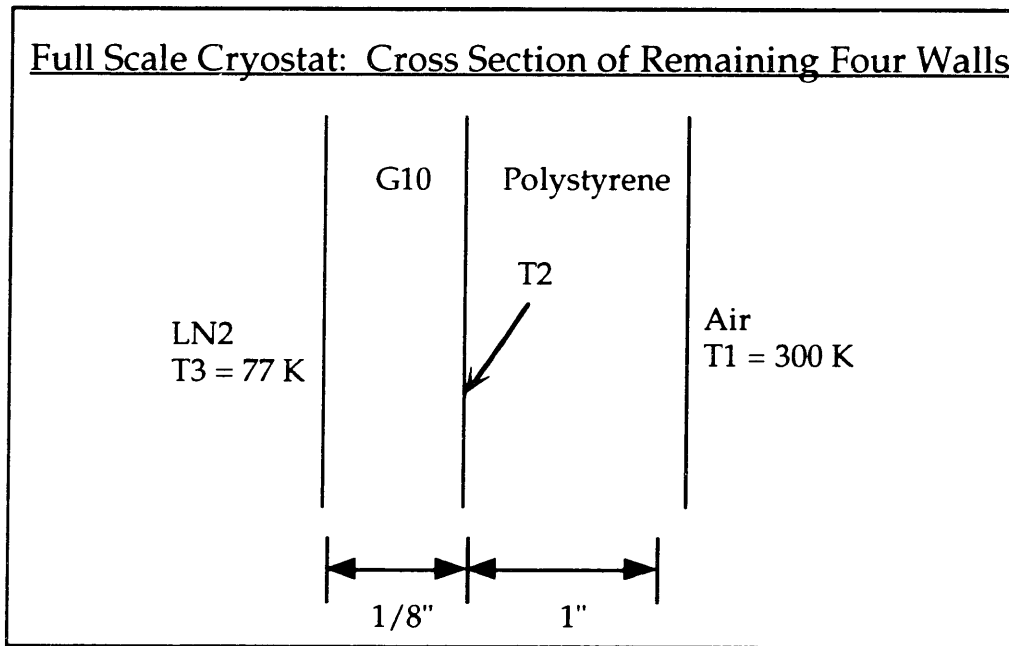

Figure 21: Cross section of the left, right, rear and top walls of the full scale cryostat.

Applying Equation 6 to this cross section, the interface temperature is determined to be $T_2 = 78.09$ K. The total area of the four walls is $A_4 = 0.26$ m^2, and the power dissipation is:

$$P_5 = 49.97 \text{ watts}$$

Therefore, the total power dissipation through the walls of the full scale cryostat, due to thermal conduction, is:

58

$$P_T = P_1 + P_2 + P_3 + P_4 + P_5$$
$$= 6080.40 + 11.49 + 101.32 + 7.77 + 49.97$$
$$P_T = 6250.95 \text{ watts}$$

9. References

[1]   Gerhart, P. M., Gross, R. J., and Hochstein, J. I. Fundamentals of Fluid Mechanics, second edition. Addison-Wesley Publishing Company, Reading, Massachusetts, 1992.

[2]   Incropera, F. P. and De Witt, D. P. Fundamentals of Heat and Mass Transfer, third edition. John Wiley & Sons, New York, 1990.

[3]   Iwasa, Y. Case Studies in Superconducting Magnets. Plenum Press, New York, 1994.

[4]   Lide, D. R. (ed.) CRC Handbook of Chemistry and Physics, 72nd edition. CRC Press, Inc., Boston, 1991.

[5]   Senturia, S. D. and Wedlock, B. D. Electronic Circuits and Applications. John Wiley & Sons, New York, 1975.

[6]   Thompson, M. T. "Design and Test of an Iron Core High Temperature Superconducting Magnet for MAGLEV," first draft. Ph. D. thesis, December 1994, Laboratory for Electromagnetic and Electronic Systems, MIT.

[7]   User's Practical Selection Handbook for Optimum Plastics, Rubbers, and Adhesives. Compiled by The International Technical Information Institute, 1976.